

Running head: MIXED PROCESS, HUMID-TROPICAL, SHORELINE–SHELF
DEPOSITION

**MIXED PROCESS, HUMID-TROPICAL, SHORELINE–SHELF DEPOSITION AND
PRESERVATION: MIDDLE MIOCENE–MODERN BARAM DELTA PROVINCE,
NORTHWEST BORNEO**

DANIEL S. COLLINS^{1*}, HOWARD D. JOHNSON¹, PETER A. ALLISON¹, and ABDUL
RAZAK DAMIT²

*¹Department of Earth Science and Engineering, Prince Consort Road, Imperial College
London, South Kensington, London, SW7 2BP UK*

²No. 9. Simpang 265-254, Kampong Bukit Bunga, Jerudong, Brunei Darussalam

*corresponding author e-mail: dscollins.geo@gmail.com

Keywords:

Mixed-process, shoreline–shelf, coastal–deltaic, humid-tropical, preservation

ABSTRACT

This evaluation of the Miocene–Modern Baram Delta Province (BDP) depositional system provides: (1) a rare case study of outcrop observations that can be directly compared with a closely comparable and geographically adjacent modern analogue; (2) new insights into how deposition and preservation occur across a range of process regimes in a highly aggradational tectono-stratigraphic setting; and (3) an example of a well-exposed mixed-influenced shoreline–shelf depositional system, displaying variable interaction of fluvial, wave and tidal processes. The exceptionally close relationship between the present-day BDP source-to-sink system and its ancient (Miocene–Pliocene) counterpart is because the climatic (humid-tropical, ever-wet, monsoon-influenced), tectonic (active foreland margin), hydrological (multiple, relatively short rivers), and gross depositional (shoreline–shelf) settings have remained consistent over the past c. 15–20 Myr. This study compares exposure-based analyses of facies and stratigraphic architecture in the Middle Miocene Belait Formation (eastern BDP) with process-based geomorphological and sedimentological analyses of coastal–deltaic depositional environments in the present-day BDP. The Belait Formation comprises three distinct types of vertical facies-succession sets: (1) Aggradationally-stacked, upward-sanding units (10–50 m thick), dominated by erosionally based sandstone beds showing swaly cross-stratification and gutter casts, record deposition during simultaneously high storm-wave energy and storm-enhanced fluvial discharge (“storm floods”); these are interpreted as analogs for deposits along the present-day open coastline in the BDP (e.g., the present-day, open-shelf Baram delta and flanking strandplain); (2) Aggradationally stacked, heterolithic, upward-sanding units characterized by interbedded swaly cross-stratified sandstone and combined-flow-rippled heterolithics, record deposition by time-varying storm and storm-flood processes under relatively high fluvial influence; these compare favorably with deposits along the present-day low-wave-energy, embayed deltaic coastlines in the BDP

(e.g., Trusan delta and other bayhead deltas in eastern Brunei Bay); (3) Heterogeneous successions comprising heterolithic, variably bioturbated and carbonaceous-rich, mudstone-dominated and muddier- to sandier-upwards units, document highly variable mixed-process deposition; these are similar to the present-day fluvio-tidal deposits along embayed deltaic coastlines in the BDP (e.g., northern Brunei Bay and Inner Brunei Bay in the southwest). The principal controls on large-scale (100–1000s m) ancient stratigraphic architecture and changes in process regime in the BDP were: (1) sediment-supply variation along the multiple river-sourced coastal plain, mainly caused by tectonically driven drainage-basin switching; and (2) formation of tectonically controlled embayments.

INTRODUCTION

Shoreline–shelf (including “shallow-marine” and “coastal-deltaic”) depositional systems are governed by the interaction of autogenic and allogenic controls that determine coastal morphology and sedimentary characteristics, including the following: plate-tectonic setting, climate, hinterland geology, drainage-basin size, sediment supply, sediment caliber, base-level fluctuations, ocean-basin morphology, hydrodynamics, and shelf width (e.g., Short 2006; Ainsworth et al. 2011; Nyberg and Howell 2016). Initially, modern shorelines were classified as wave-, river- or tide-dominated (e.g., Coleman and Wright 1975; Galloway 1975; Zaitlin et al. 1994). However, at least one-third of modern depositional shorelines display mixed-process morphologies (Nyberg and Howell 2016). For ancient shoreline–shelf depositional systems, there has been an increase in the identification of different process signals and mixed-process depositional systems, including their spatial and temporal variability (e.g., Buatois et al. 2008; MacEachern and Bann 2008; Ainsworth et al. 2011; Buatois et al. 2012; Vakarelov et al. 2012; Legler et al. 2014; Shiers et al. 2014; Ainsworth et al. 2015; Li et al. 2015; Gomis-Cartesio et al. 2016; Gugliotta et al. 2016a; Gugliotta et al. 2016b; Rossi and Steel 2016; van Cappelle et al. 2016; van Cappelle et al. 2017). However,

comparing ancient depositional environments and processes from the sedimentary record with their modern counterparts is limited by: (1) the extent to which modern depositional environments and their physical processes are truly analogous of ancient systems; and (2) the preservation potential of modern sedimentary deposits (e.g., Dott 1983; Thorne et al. 1991; Miall 2015; Nyberg and Howell 2015). This study focuses on shoreline–shelf deposits from Miocene successions in the Baram Delta Province (BDP), northwest Borneo (Fig. 1), where a shoreline–shelf depositional system has operated for the past 15 Myr, and continues today, along a humid-tropical and active foreland margin (Sandal 1996; Hall and Nichols 2002; Morley and Back 2008). Consequently, modern shoreline–shelf environments and their depositional processes provide a remarkably close and well-constrained analogue to the Miocene–Pliocene period, and *vice-versa* (Collins et al. 2017).

The aims of this paper are as follows: (1) to describe and interpret process facies signals and stratal architecture in the Middle Miocene Belait Formation, onshore eastern BDP; (2) to undertake a process-based geomorphological and sedimentological analysis of present-day depositional systems in the BDP and compare this with ancient sedimentary facies; (3) to develop a depositional model that integrates the ancient and modern systems, and enables comparison of the BDP depositional system with other ancient and modern examples; and (4) to discuss the controls on the architecture and preservation of strata in shoreline–shelf systems.

GEOLOGIC SETTING

Ancient

The BDP is located in the much larger Baram–Balabac Basin along the active foreland margin of the southern South China Sea (SCS) (Fig. 1A). To the southeast (Fig. 1B), the Eocene–Oligocene deep-water clastic deposits of the Rajang–Crocker Range hinterland have

been intermittently uplifted and exhumed (> 5 km) throughout the Neogene (Levell 1987; Sandal 1996; Hall and Nichols 2002; Morley and Back 2008). The erosional products have formed up to 9–12 km of mainly progradational to strongly aggradational shoreline–shelf deposits in the BDP (e.g., Sandal 1996). The high rate of subsidence (up to 3000 m/Myr; Sandal 1996) is a result of loading by deltaic sediments and consequent reactivation of basement-linked faults (e.g., Morley et al. 2003; Gartrell et al. 2011).

The onshore Belait Formation represents the proximal, Middle–Late Miocene basin fill of the eastern BDP, but their biostratigraphic ages are imprecisely known (Simmons et al. 1999).

The study area is located in a sub-basin of the BDP, the Berakas Syncline (Fig. 1B, C). The Berakas Syncline was initiated as a tectonically active sub-basin during the Middle Miocene, and was subsequently further deformed into its present form during the Late Miocene to Pliocene. The broad synclinal structure of the Berakas Syncline is bounded by two basin-bounding faults that were reactivated during Late Miocene–Pliocene compression into their present form, comprising reverse faults (the Jerudong and Muara faults; Fig. 1C) and associated tight inversion anticlines (Morley et al. 2003; Gartrell et al. 2011).

Modern

The Modern BDP source-to-sink system (Fig. 1B) is characterized by the following: (1) a narrow and steep coastal plain (< 100 km, c. 1°) and shelf (< 100 km, c. 0.1°) (Hiscott 2001); (2) several, independent, small-sized (10^2 – 10^5 km²) drainage basins; (3) suspended-sediment-dominated fluvial discharge; (4) fluvial bedload sand transport during high discharge, which is linked to monsoonal storms (Douglas et al. 1999; Dykes 2000); (5) wave-dominated, river- and tide-influenced, open-coastline deposition (Lambiase et al. 2002), and (6) more variable, mixed-energy deposition in embayed coastal areas (e.g., Brunei Bay) (Abdul Razak 2001).

METHODS AND DATASET

Ancient Facies Analysis

Facies analysis was undertaken on exposures of the Belait Formation in the Berakas Syncline of eastern Brunei (Fig. 1B, C). Exposures are relatively small ($< 100 \text{ m}^2$); they were created during civil-engineering projects, but they are of extremely high quality in terms of defining millimeter- to decimeter-scale sedimentary features, lithofacies characteristics, biogenic features and ichnofauna (following the schemes of Reineck (1963), Taylor and Goldring (1993), Taylor et al. (2003), and MacEachern and Bann (2008)). Exposures were GPS-located and studied using integrated datasets comprising logged sections (1:50 scale), detailed photomontages, and field sketches. Facies were grouped into facies successions, equivalent to parasequences (*sensu* Van Wagoner et al. 1990), and facies successions were grouped into facies-successions sets, equivalent to parasequence sets (*sensu* Van Wagoner et al. 1990). Process interpretations for facies successions and succession sets were qualitatively assessed based on the relative proportions of facies and the general process interpretations of facies, their primary sedimentary structures, and other facies characteristics (Ainsworth et al. 2011).

Geomorphological Analysis

Depositional environments, alternatively termed element complex sets (Vakarelov and Ainsworth 2013), were interpreted based on planform geomorphological analysis using satellite imagery (Google Earth) and aerial photographs, and involved the recognition and process-based interpretation of groups of depositional elements (Ainsworth et al. 2011; Nanson et al. 2013). Additional data also included regional-scale bathymetric maps and smaller-scale (tens of km^2) surveys produced using a single-frequency echo sounder (Abdul Razak 2001).

Present-Day Sediment Coring and Sedimentological Analysis

A total of 135 sediment vibracores were collected in the western Brunei Bay using a 4" diameter and 1-m-length core barrel (Abdul Razak 2001). Core locations were GPS located and sediment cores were slabbed and dried for sedimentological analyses, which included grain size, lithology, organic-carbon content, and bioturbation. No other sediment cores are available from the present-day BDP. The median and maximum grain size of offshore sediment grab samples is available from the central to western BDP (James 1984; Sandal 1996).

FACIES ANALYSIS

Eleven facies have been defined at the centimeter to meter scale (F1–F11 in Table 1). These have been grouped into nine facies successions covering the meter to decameter scale (FS 1–FS 9 in Table 2), which are summarized below and supplemented by representative sedimentological logs and photographs (Figs. 2–10 and Supplementary Fig. 1A-I). The c. 200 m of logged sections presented here come from a total of c. 964 m of measured stratigraphy.

FS 1: Sandier-Upwards, Mudstone-Dominated to Sharp-Based, Swaly Cross-Stratified, Sandstone-Dominated Units

Description.—Facies succession 1 comprises 10–50 m thick, sandier-upward units (Fig. 2A–D). A basal, 5–20 m thick, mudstone-dominated (> 80%) part comprising laminated (F3) and massive (F2a) silty mudstones and sharp-based, < 5 cm thick, siltstone beds (F6, F10a) are gradationally or sharply overlain by 3–20 m thick heterolithic units with interbedded sharp-based, 0.25–0.8 m thick sandstone and 5–20 cm thick muddy heterolithics (F4a; Fig. 2A, B). Sandstone beds are very fine-grained and dominated by long-wavelength (c. 4–16 m), low-angle (< 15–20°), swaly cross-stratification (SCS; F6) with common, millimeter-thick mud and carbonaceous drapes. Gutter casts are abundant and geometrically variable with decimeter- to meter-scale widths and thickness (Fig. 2C, D) (Collins et al. 2017). Subordinate

sandstone facies display hummocky cross-stratification (HCS; F7) and quasi-planar lamination (F8a; Arnott 1993). The upper sandstone-dominated (> 80%) units (2–18 m thick) comprise 1–3.6 m thick bedsets of SCS-dominated, very fine-grained sandstone (F6) and minor (< 20%), thin (< 10 cm thick) mudstone-dominated units (F2a, F3, F4a).

Bioturbation in the sandstones is generally low (BI 0–1), with higher intensity (BI 1–3) near bed tops; *Ophiomorpha* dominates, with less abundant *Asterosoma*, *Palaeophycus*, *Planolites*, and *Rosselia*, which constitutes an impoverished *Skolithos* ichnofacies (Buatois et al. 2008; MacEachern and Bann 2008; Buatois et al. 2012). Bioturbation in mudstone-dominated facies is more variable (BI 0–5): ichnofauna include *Chondrites*, *Palaeophycus*, *Planolites*, and *Thalassinoides* with less common *Asterosoma*, *Cylindrichnus*, *Phycosiphon*, *Rosselia*, and *Schaubcylindrichnus*, which corresponds to a slightly impoverished *Cruziana* ichnofacies (MacEachern and Bann 2008).

Interpretation.—Mud deposition can occur under both high-energy flows (e.g., Schieber et al. 2007; Plint 2014; Baas et al. 2016) and during quiet-water suspension settling (e.g. Howard and Reineck 1981). Unbioturbated, structureless mudstones (F2a) may reflect fluid-mud deposition (Plint 2014), while laminated silty mudstones (F3) may reflect deposition by turbulent–laminar, mixed clay–silt flows (Baas et al. 2016). Associated combined-flow-rippled siltstones and sandstones showing SCS, suggests oscillatory-dominated, combined-flow deposition during storms; hence deposition was above storm wave base (SWB) (e.g., Dumas et al. 2005; Plint 2014). Interbedded sandstone- and mudstone-dominated facies is consistent with fluctuating sand supply during storms (Thorne et al. 1991). In the humid-tropical BDP, storms simultaneously increase river- and storm-driven sediment supply during “oceanic floods” (Wheatcroft 2000) or “storm floods” (Bhattacharya 2005; Collins et al. 2017). Fluvial influence is supported by the intimate association of carbonaceous material and mudstone within (drapes and clasts) and between sandstone beds. A mixed fluvio-marine

setting is also consistent with the impoverished *Cruziana* ichnofacies and the overall low intensity of bioturbation (MacEachern and Bann 2008).

Consequently, FS 1 is interpreted to reflect open marine deposition in a wave-dominated, river-influenced, 'storm flood'-dominated delta and/or flanking strandplain. The upward increase in sandstone bed proportion, thickness, and amalgamation most likely reflects progradation driven by an excess of sediment supply over accommodation, possibly in combination with: (1) increased storm size and frequency; (2) increased average storm energy; and/or (3) increased frequency and/or energy of the largest-magnitude storms (Storms and Hampson 2005; Sømme et al. 2008; Charvin et al. 2011).

FS 2: Sandier-Upwards, Variably Bioturbated, Heterolithic to Swaly Cross-Stratified, Sandstone-Dominated Units

Description.—Facies succession 2 comprises 2–8 m thick, sandier-upwards units with a basal, 1–3 m thick part comprising massive (F2a) and laminated (F3) mudstones that pass gradationally or sharply upward into a 1–5 m thick interval of interbedded muddy and sandy heterolithics (F4a, F5a) and sandstone beds (F6, F7) (Figs. 2E–H, 3). Heterolithic facies contain centimeter-thick, sharp-based siltstone–sandstone beds displaying combined-flow ripples with variable asymmetry and common, but variable, mud and/or carbonaceous drapes (Fig. 2E, G, H). These fine-grained drapes lack any systematic stratigraphic organization, and paired or rhythmic drapes are absent. Interbedded sharp-based, very fine-grained sandstone beds (0.1–0.9 m thick) and bedsets (0.5–5 m thick) display occasional gutter casts, generally asymmetric SCS (F6) and low-angle planar lamination (F9a), with common mud and carbonaceous laminae and clasts, and occasional climbing combined-flow ripples (Figs. 2G, H, 3). Subordinate facies include: (1) decimeter-thick and meter-wide lenses of fine-grained sandstone displaying bidirectional trough cross-bedding with mud-draped toesets and

mudstone lags (F9a; Figs. 2H, 3); (2) mudstone- and coal-intraclast conglomerates (F11a; Fig. 3); and (3) bidirectional-current-rippled sandstones (F10b).

Bioturbation in heterolithic and sandstone facies is highly variable (BI 0–5), sporadic, and dominated by stratification-crossing elements (Bann et al. 2008), most commonly *Palaeophycus*, *Planolites* and *Ophiomorpha*, and/or *Thalassinoides*. There are less common occurrences of *Asterosoma*, *Bergaueria*, *Cylindrichnus*, *Phycosiphon*, *Rosselia*, and *Skolithos* (Fig. 2E). This assemblage constitutes a slightly impoverished *Cruziana* ichnofacies. More rarely, units are pervasively bioturbated by *Thalassinoides* and less common *Chondrites*, *Diplocraterion*, *Palaeophycus*, *Planolites*, and *Rosselia* (Fig. 2F).

Interpretation.—The abundance of combined-flow-rippled, heterolithic facies suggests strong variability in both sediment supply and hydrodynamic energy of mixed mud–sand combined flows, probably related to combined storm and fluvial processes (storm floods) (MacKay and Dalrymple 2011; Plint 2014; Baas et al. 2016; Collins et al. 2017).

Compared to FS 1, SCS-dominated beds in FS 2 are thinner, contain a higher proportion of interstratified heterolithics, and contain fewer gutter casts, which suggests a more distal depositional setting. In this context, these differences could reflect: (1) decreased storm strength and/or frequency; and (2) increased rate of sedimentation and/or thickness of preserved sedimentation between successive “gutter-forming” storm floods. The lack of symmetrical ripples in heterolithic and sandstone facies suggests minor fairweather reworking, which could reflect: (1) open-marine deposition below fairweather wave base (FWWB); (2) open-marine deposition above FWWB but under low-energy fairweather conditions; or (3) deposition in a region protected from waves. Bidirectional current indicators and mud drapes in subordinate fine-grained sandstones suggest relatively minor tidal influence which, in addition to storm waves, currents, and river-related flows, may have

contributed to the abundance of combined-flow-ripple cross-lamination. There may have been an additional grain-size control on process preservation (e.g., Yoshida et al. 2007).

The heterogeneous lithology, high suspended-sediment concentration, and marine-dominated conditions during deposition of FS 2 are evidenced by a sporadic but relatively diverse bioturbation (Bann et al. 2008; MacEachern and Bann 2008). However, the predominance of facies-crossing ichnotaxa and the relative paucity of grazing structures attests to a high degree of infaunal opportunism in a depositional setting prone to physiological stress (MacEachern and Bann 2008). Intensely bioturbated, *Thalassinoides*-dominated ichnofabrics most likely suggest periods of decreased sedimentation rate. The dominance of *Thalassinoides* suggests salinity fluctuations, which present-day crustaceans that create *Thalassinoides*-like burrows can tolerate {Stanzel, 2004 #875}.

Overall, FS 2 is interpreted to record progradational, mixed-energy, wave-dominated, river-influenced and tide-affected deposition in a relatively low wave-energy, open-marine or embayed setting, including delta-front, mouth-bar, and/or lobe environments (Vakarelov and Ainsworth 2013).

FS 3: Sandier-Upwards, Muddy to Sandy Heterolithic Units

Description.—Facies succession 3 consists of 2–8 m thick, sandier-upwards units (Fig. 4A). Complete successions change gradually upward from structureless (F2a) and/or laminated mudstone (F3), through muddy to sandy heterolithics (F4b, F5b) (e.g., Fig. 4A), current-rippled very fine-sandstone (F10b) and laminated sandstones (F8d), and into trough cross-bedded very fine-grained sandstone (F9b).

Muddy heterolithic facies (F4b) are lenticular to wavy bedded, comprising > 50% laminated (F3) and massive (F2a) silty mudstone with subordinate centimeter-thick beds of very fine-grained sandstone (Fig. 4B). The latter most commonly display combined-flow-ripple (F10a)

or modified-current-ripple (F10b) cross-lamination. Sandy heterolithic facies (F5b) are wavy to flaser bedded, comprising > 50%, centimeter-thick, very fine-grained sandstone beds with bidirectional cross-lamination (Fig. 4C). Mudstone facies (F2a, F3) also form 0.1–2 cm thick drapes within and across ripple laminae sets (Fig. 4C, D).

Sandy heterolithics, in units up to 6 m thick (Fig. 4A), show gradual vertical and lateral transitions with interbedded lenses (decimeter-thick and meter-wide) and more continuous beds of bidirectional trough-cross-bedded sandstone (F9b), laminated sandstone (F8d), and swaly-cross stratified sandstone (F6) with common mud and carbonaceous drapes, laminae, and clasts (Fig. 4D, E). Facies 9b also forms amalgamated bedsets up to 3 m thick.

Carbonaceous debris, including centimeter-scale coal clasts, is common throughout all facies.

Bioturbation in FS 3 is generally low (BI 1–2), but localized areas (decimeter-scale) display intense bioturbation (BI 3–5). Small, facies-crossing ichnotaxa dominate, including *Asterosoma*, *Gyrolithes*, *Ophiomorpha*, *Palaeophycus*, *Planolites*, *Rosselia*, *Teichichnus*, and *Thalassinoides* (Fig. 4B, C). Compound escape structures (fugichnia) form decimeter-scale “lam-scam” areas (Gingras et al. 1998).

Interpretation.—Heterolithic facies indicate deposition under fluctuating sediment supply and hydrodynamic conditions. Bedload sand transport occurred mainly as current ripples, and bidirectional paleocurrents suggest tidal influence. Mud deposition could reflect deposition under: (1) low-energy, relatively low concentration, suspension fallout during low flow and slack-water tides; and (2) high-energy turbulent–plug flows (MacKay and Dalrymple 2011; Baas et al. 2016). Tropical river floods supply high volumes of both bedload and suspended sediment; therefore, flood–interflood cyclicality was probably a major cause of heterolithic sedimentation (e.g., Gugliotta et al. 2016b). Exquisitely preserved sand–mud lamination suggest a high sedimentation rate during floods.

Sporadic stratification-crossing ichnogenera indicate a variable sedimentation rate, and their small-size suggests reduced salinity, both consistent with river-influenced deposition (MacEachern and Bann 2008). The low-diversity *Cruziana* to *Skolithos* ichnofacies has been observed in interpreted ancient environments, including interpreted tide-dominated delta fronts (Willis et al. 1999; MacEachern et al. 2005; Legler et al. 2013) and tide-influenced embayments (Buatois et al. 2012), crevasse subdeltas (Gugliotta et al. 2015), and distributary channels (Buatois et al. 2012). The thicknesses of FS 3 units are similar to those of modern and ancient tidal bars and deltas (Legler et al. 2013; Gugliotta et al. 2015). Tropical intertidal regions in the Miocene BDP would have been densely vegetated by mangroves, as seen in analogous modern environments (e.g., Brunei Bay; Fig. 1B) (e.g., Abdul Razak 2001). Hence, FS 3 deposition occurred in subtidal, tide- and river-influenced bars and delta fronts, in a partly restricted (low wave energy) coastal embayment (e.g., Trusan delta in Brunei Bay; Lambiase et al. 2003).

FS 4: Upward-Coarsening, Sparsely Bioturbated, Sandstone-Dominated Units

Description.—Facies succession 4 consists of 3–5 m thick, sandier- and coarsening-upward units. Complete successions comprise laminated mudstone (F3) with very fine-grained sandstone laminae, passing upwards through interbedded laminated mudstone and 3–30 cm thick, very fine-grained sandstone beds (F8c–d, F9c), and into up to c. 3-m-thick sandstone bedsets displaying trough cross-bedding (F9c), planar lamination (F8c–d), current ripples (F10c), and minor SCS (F6). Cross-lamination and cross-bedding are typically unidirectional and occasionally show millimeter-scale mud and carbonaceous drapes and symmetrical cross-lamination. Sandstone bed bases are typically sharp, often with decimeter-scale gutter casts, and with granule–pebble lags of mudstone and carbonaceous debris.

Bioturbation is sparse (BI 0–1) and dominated by simple, small *Palaeophycus* and *Planolites*, with subordinate *Ophiomorpha* and *Skolithos*.

Facies succession 4 is rare in the studied exposures but is more common in the lower Belait Formation on Labuan (Fig. 1B) (e.g., Madon 1994), where soft-sediment deformation (e.g., slumps and debrite beds) is common (F1).

Interpretation.—The mainly unidirectional, current-dominated cross-lamination and cross-bedding confirms bedload transport by currents. The strongly heterolithic character and sharp bed bases indicate episodic erosion and deposition. Gutter casts, SCS, and symmetrical ripples indicate some oscillatory-dominated reworking. The low diversity and small size of ichnofauna indicates environmental stress, such as reduced salinity, high sedimentation rate, water turbidity, and/or episodic deposition (MacEachern and Bann 2008). Soft-sediment deformation suggests high sedimentation rate, slope instability, and rapid dewatering. The upward-sanding trend suggests delta progradation due to an excess of sediment supply over accommodation, shallowing, and/or increased frequency of tractional flows (e.g. Orton and Reading 1993). Consequently, FS 4 units are interpreted as deposition in river-dominated, wave- and storm-affected delta fronts.

FS 5: Erosionally Based, Upward-Fining, Sandstone-Dominated Units

Description.—Facies succession 5 comprises 3–5 m thick, muddier-upward successions with sharp, erosional, flat to concave-upwards bases that are commonly lined with granule- and pebble-sized, mudstone intraclasts (F11a) and, more rarely, quartzite and/or sandstone extraclasts (F11b). The overlying sandstones are lower-medium- to very fine-grained with unidirectional trough cross-bedding (F9c) and low-angle lamination (F8c–d). Cross-set thicknesses decrease upwards from 0.5–0.8 m to 0.2 m. Cosets boundaries are often low-angle sigmoidal surfaces, usually dipping in the same direction as intervening cross-sets. Facies 9c becomes intercalated upwards with very fine-grained sandstones displaying low-angle lamination (F8d) and, to a lesser extent, climbing (< 10°)-current-ripple cross-

lamination (F10c). Overlying muddy heterolithics contain bidirectional current-ripple and combined-flow-ripple cross-lamination (F4a–b) and become increasingly mud-rich (F3) upward. Minor mud and carbonaceous clasts and laminae, plus centimeter-scale coal fragments, are sporadically distributed in all facies. Sandstone facies generally lack bioturbation, but a highly impoverished *Cruziana* ichnofacies (BI 0–1) comprising small-scale *Palaeophycus*, *Planolites*, and fugichnia occur in some instances in the upper parts of some units.

Facies succession 5 is uncommon in the eastern BDP but is much more common in the approximately time-equivalent Lambir Formation in the western BDP.

Interpretation.—The basal erosional surfaces with coarse-grained lags, primary sedimentary structures indicative of unidirectional traction currents (including climbing-current-ripple cross-lamination), minor bidirectional paleocurrents, and the sparse to absent impoverished bioturbation suggest that FS 5 units were deposited under high sedimentation rates in river-dominated, tide-influenced channels (Flood and Hampson 2014; Ainsworth et al. 2015). Coset boundaries are interpreted as the downstream-accreting surfaces of large fluvio-tidal bars. The fining-upward facies successions represent either laterally migrating channels or the progressive infill of abandoned channels.

FS 6: Erosionally Based, Upward-Fining, Sandstone-Dominated to Sandy Heterolithic Units

Description.—Facies succession 6 forms 1–6 m thick upward-fining units: sandstone facies (1–5 m thick) pass gradationally upwards through sandy heterolithics (1–3 m thick) and into mudstone facies (1–3 m thick) (Fig. 5A, B). Basal surfaces are scoured, flat to concave-upward, and associated with conglomerate containing granule- to pebble-sized, mudstone intraclasts, carbonaceous debris, and, more rarely, quartzite and/or sandstone extraclasts.

Overlying very fine- to fine-grained sandstone show trough cross-bedding (F9b), low-angle lamination (F8c–d), current-ripple cross-lamination (F10b), and more minor SCS (F6) (Fig. 5C). Trough cross-sets display variable thicknesses (10–50 cm) and widths (30–150 cm) (Fig. 5C). Paleocurrent directions are predominantly towards between W and N, with a minor oppositely directed component. Coset packages are bounded by 10–20 m long, inclined (5–20°) surfaces that downlap the basal contact (Fig. 5A) and may dip approximately perpendicular, parallel, or oppositely to intervening cross-sets.

Interstratified and overlying carbonaceous-rich sandstones (F8d, F10b) and heterolithic (F4b, F5b) are similar to equivalent facies in FS 3 and often show unidirectional-current-ripple cross-lamination, generally dipping towards W–N, that may show low-angle (< 10°) climb (Fig. 5B, D, E).

Bioturbation in the sandstone facies is sparse (BI 0–1) and comprises small *Palaeophycus* and *Planolites*. Bioturbation increases in the heterolithic facies (BI 0–2, locally BI 3–5) and includes *Ophiomorpha*, *Palaeophycus*, *Planolites*, *Skolithos*, resting traces (Fig. 5D), and escape structures.

Interpretation.—The sharp basal surface reflects erosion during channel incision and lateral migration. The predominantly unidirectional paleocurrents and sparse impoverished bioturbation are consistent with river-dominated, tide-influenced deposition (MacEachern and Bann 2008). The dominant W–N paleocurrent direction is perpendicular to the general Middle Miocene shoreline orientation (Fig. 1B), which is consistent with the inferred fluvial sediment-transport direction (e.g., Sandal 1996). The upward increase in bioturbation intensity and diversity suggests progressively more tidal influence. This could reflect changes in tidal strength related to basin-scale controls (e.g., shelf width) or relatively local-scale controls (e.g., coastline morphology) (e.g., Ainsworth et al. 2011; Shiers et al. 2014). Mud

drapes and layers in both the sandstone and heterolithic facies may reflect flood–interflood cyclicity and, with increased marine influence, tides and/or mixed sand–mud transitional flows (as in FS 3) (e.g., Baas et al. 2016; Gugliotta et al. 2016b). Opposed paleocurrents support some tidal influence. Hence, FS 6 is interpreted to reflect deposition in downstream, upstream, or laterally accreting bars in river-dominated, tide-influenced channels.

FS 7: Erosionally Based, Upward-Fining, Heterolithic-Dominated Units

Description.—Facies succession 7 forms 2–6 m thick, sharp-based, fining- and muddier-upwards successions. The flat to concave-upward base and associated mudstone intraclast conglomerates are overlain by laminated (F8c–d) and trough cross-bedded (F9b), fine- to very fine-grained sandstone (up to 5 m thick; Fig. 5F, G). Compound, shovel-shaped, 10–50 cm thick cross-sets generally dip towards the NW–N, with a subordinate orientation towards the SE–S, and thin down-dip into similarly bidirectional-current-rippled, muddy to set heterolithics (F4b, F5b; Fig. 5F). Structureless, 0.2–2 cm thick mud drapes on foresets, reactivation surfaces and to set ripples, and mud rip-up clasts and carbonaceous debris are common (Fig. 5F). Meter-scale, low-angle ($< 10^\circ$) surfaces form to set and/or bed boundaries. The intercalated and overlying sandy (F5b; 1–2 m thick) and muddy heterolithics (F4b; 1–3 m thick) share similar characteristics to those of their equivalent facies in FS 3, including bidirectional current ripples and mud drapes.

Bioturbation in sandstone facies (BI 0–1) is of low diversity and dominated by *Ophiomorpha*, *Palaeophycus* and *Planolites*. Bioturbation in heterolithic facies (BI 0–3, locally BI 4–5) contains *Ophiomorpha*, *Palaeophycus*, *Planolites*, *Teichichnus*, and “lam-scram” (Gingras et al. 1998).

Interpretation.—Bidirectional paleocurrents, mud drapes and bioturbation, and the paucity of wave-related features suggests tide-dominated deposition (e.g., Nio and Yang 1991).

However, fluvial influence is implied by the variable grain size, dominant basinward paleocurrent direction, abundance of mud, lack of systematic mud drape bundling, and low to moderate ichnofauna diversity and bioturbation intensity (MacEachern et al. 2005; MacEachern and Bann 2008; Gugliotta et al. 2016b). The erosional base, fining-upward facies trend and heterolithic character are consistent with tide-dominated channel deposition, close to the turbidity-maximum zone, down-dip of the fluvial–tidal transition (e.g., Dalrymple and Choi 2007). Trough-cross-bedded sandstone formed as migrating subaqueous dunes, which probably passed laterally (off channel axis) into smaller bedforms (Legler et al. 2013).

Facies succession 7 closely resembles other examples of interpreted tide-dominated channel fills (e.g., in the Eocene Dir Abu Lifa Member, Egypt; Legler et al. 2013). Hence, the inclined accretion surfaces may preserve: (1) downstream-accreting, mid-channel tidal bars; (2) laterally accreting, side-attached tidal bars; and/or (3) point bars (Legler et al. 2013).

The upward trend of decreasing grain size, sand content, and bedform scale, and increasing mud content and bioturbation, is consistent with a decrease in tidal energy and fluvial influence during channel infill.

FS 8: Laminated to Massive Mudstone Units with Sandy Interbeds

Description.—Facies succession 8 forms 3 to > 40 m thick, mudstone-dominated units dominated by poorly bioturbated (BI 0–2) laminated mudstones (F3) and massive mudstones (F2a) with abundant, indistinct bioturbation (BI 4–5) (Fig. 5H). Heterolithic facies (< 40%) contain centimeter-thick, very fine- to fine-grained sandstone beds showing current, combined-flow, and minor symmetrical-ripple cross-lamination (F4, F5; Fig. 5H). The vertical distribution of heterolithic facies may define 1–3 m thick, upward-sanding units and, more rarely, 1–2 m thick, sharp-based, muddier-upwards units. Occasional sharp-based, 0.2–

1 m thick beds show SCS, minor HCS, and gutter casts (F6, F7). Drapes and clasts of mud and carbonaceous material, including abundant mangrove pollen (Simmons et al. 1999), are ubiquitous throughout all facies. Bioturbation in the heterolithic facies (BI 1–2) includes *Ophiomorpha*, *Palaeophycus*, *Thalassinoides*, and possible dwelling burrows (Fig. 5H).

Interpretation.—Mudstone dominance suggests deposition in a distal and/or lateral setting relative to the main fluvial and/or wave-driven sand supply. Laminated mudstones may reflect low- or high-energy deposition (see FS 1). The variable-intensity, low-diversity bioturbation suggests variable deposition rates in a stressed, marine-influenced environment (MacEachern and Bann 2008). Predominance of current-ripple cross-lamination suggests deposition in a tide- and/or river-influenced, low-wave-energy environment. Swaly cross-stratified sandstones probably record infrequent storm floods (Collins et al. 2017). Possible depositional environments include (1) interdistributary bays, (2) open-marine bays, (3) muddy estuaries, and (4) abandoned tidal creeks and channels (e.g., when overlying sharp basal surfaces) (MacEachern and Bann 2008). Abundant mangrove pollen is consistent with marginal-marine, tidal deposition (Simmons et al. 1999).

FS 9: Massive, Carbonaceous Mudstone Units

Description.—Facies succession 9 forms 3–10 m thick units dominated (> 90%) by carbonaceous and mangrove-pollen-rich (Simmons et al. 1999), massive mudstone (F2b). Organic debris is pervasive and includes (1) millimeter-scale flakes and fibers, (2) millimeter- to centimeter-scale coal fragments, and (3) rare *in-situ*, decimeter-scale coals (Fig. 5G) and coalified roots (Fig. 5I). Decameter-scale, very fine- to fine-grained sandstone units are extremely mottled and lack stratification (Fig. 5J). Bioturbation is generally indistinct but includes *Thalassinoides*-like burrows (cf. Fig. 5H). Facies succession 9 typically overlies FS 8 to form > 10 m thick, muddier-upwards successions or abruptly overlies FS 7.

Interpretation.—Carbonaceous-rich, bioturbated mudstone, with abundant mangrove pollen and the association with FS 8, suggests subtidal–intertidal deposition on a mangrove-fringed lower coastal plain, probably in a low-wave-energy coastal embayment (Amir Hassan et al. 2013). Sharp basal contacts with FS 7 also suggests infill of abandoned fluvio-tidal channels by mangrove swamps (Simmons et al. 1999).

Coals are rarer than in equivalent facies in the Early Miocene Nyalau Formation, northwest Borneo (Amir Hassan et al. 2013). This may reflect transgressive reworking and/or more limited mangrove development due to decreased tidal strength relative to wave and fluvial processes and/or a higher subsidence rate.

MIXED-PROCESS STRATAL ARCHITECTURE

The preceding facies analysis has identified nine facies successions (parasequences; *sensu* Van Wagoner et al. 1990) that accumulated in a variable, mixed-energy, shoreline–shelf setting (Fig. 6A): (1) FS 1 is extensively storm-wave reworked, whereas FS 2 is more mixed-process; (2) FS 3–FS 4 (deltas and/or bars) and FS 5–FS 7 (channels) are variably tide- or river-dominated; and (3) FS 8–FS 9 are tide-dominated.

The architectural relationships of the seven dominant facies successions (FS 1–FS 3 and FS 6–FS 9) are characterized by three distinctive facies successions sets (FSS; parasequence sets; *sensu* Van Wagoner et al. 1990), which reflect a range of mixed-process, and probably contiguous, shoreline–shelf environments (Figs. 6B, 7): (1) FSS 1 represents a wave-dominated (storm-wave-reworked) delta and/or flanking strandplain (Fig. 7A); (2) FSS 2 is a mixed-process (wave-, river- and tide-influenced) delta and/or flanking strandplain (FS 2) (Fig. 7B); and (3) FSS 3 is a tide-dominated, wave- and river-influenced embayment (Fig. 7C).

Facies succession set 1 is typically 60–200 m thick and comprises aggradationally stacked, 10–50 m thick, wave-dominated delta and/or flanking strandplain (FS 1) parasequences (Figs. 7A, 8A) (Atkinson et al. 1986; Johnson et al. 1989; Hadley et al. 2006). Sharp facies transitions in FS 1 units are erosional discontinuities that may have formed by increased wave and/or storm energy and/or minor relative-sea-level (RSL) fall (Dott and Bourgeois 1982; Hampson and Storms 2003; Storms 2003). Sharp or gradational transitions between successive FS 1 parasequences are most likely to represent abrupt or gradual rises in RSL, respectively (e.g., Van Wagoner et al. 1990; Hampson and Storms 2003). Subordinate units at the top of FS 1 parasequences comprise fluvio-tidal channels (FS 6), deltas and/or bars (FS 3) and embayments (FS 8), which are gradationally overlain by wave-dominated units (FS 1) (Figs. 8A, 9A, B).

Facies succession set 2 comprises aggradationally stacked, 3–15 m thick, mixed-process delta and/or flanking strandplain (FS 2) parasequences that may be over 50 m in thickness (Figs. 7B, 8B). Erosional discontinuities within FS 2 parasequences are common (Figs. 8B, 9C). However, the boundaries between successive FS 2 units are usually gradational (units 1–4, Figs. 8B, 9C), but occasionally sharp (unit 5, Figs. 8B, 9C), with the latter associated with bioclast-rich layers and intense bioturbation. Subordinate facies successions are erosionally based fluvio-tidal channels (FS 6) and tide-dominated embayments (FS 8–FS 9) (Figs. 8C, 10A–C). Mixed-process deltas and/or flanking strandplains (FS 2) may abruptly overlie erosional surfaces, which often show precursor gutter casts (e.g., 20 m, Figs. 8C, 10A–C), and may occur within multi-story channel bodies (c. 20–41 m, Figs. 8C, 10A–C). This suggests that FS 2 was deposited along mixed-process deltaic shorelines with multiple coeval fluvio-tidal channels.

Facies succession set 3 contains a variety of facies successions and architectural relationships that suggest accumulation in a low wave-energy, tide-influenced embayment (Fig. 7C). Tide-

and wave-dominated heterolithics (FS 8) are gradationally interstratified with carbonaceous-rich mangrove mudstones (FS 9) (Figs. 8D, 10D), tidal bars and/or deltas (FS 3) (Fig. 8D) and may sharply or gradationally overlie fluvio-tidal channels (FS 6–FS 7) (Fig. 8D).

Mangrove mudstones abruptly overlie tide-dominated channels (FS 7) (Figs. 8D, 10A, B, C, D). Tidal-channel sand bodies identified in offshore subsurface data in the BDP are 150–500 m wide and form multi-story channel bodies up to 20 m thick (Hadley et al. 2006). Sharp, erosional channel bases (FS 6–FS 7) suggest channel erosion, which may reflect autogenic channel switching or RSL fall (e.g., van Cappelle et al. 2016). A candidate for a major sequence boundary (e.g., Catuneanu 2006) is the base of a fluvial–tidal channel marked by well-rounded quartzite cobbles (Fig. 10D, E). The overlying succession passes gradually from stacked tidal bars (FS 3) into mixed-process delta and/or flanking strandplain units (FS 2) (Figs. 8D, 10D F), which supports its interpretation as the transgressive infill of a drowned incised valley (e.g., Zaitlin et al. 1994; Yoshida et al. 2004). Facies succession sets 2 and 3 are commonly interstratified with gradual stratigraphic transitions (Figs. 8C, 10A, B). This favors gradual spatial and temporal shifts between coeval delta and/or flanking strandplains and relatively low-wave-energy embayments in a mixed-process shoreline–shelf setting.

In summary, the three facies successions sets reflect deposition and preservation in mixed-energy shoreline–shelf depositional systems, but with contrasting behavior and coastal morphologies: (1) two types of coastal–deltaic progradation (FSS 1 and FSS 2); and (2) coastal embayment infill during depositional transgression (FSS 3). There is also a close relationship between these vertical facies successions sets and variability in reservoir quality, thickness, continuity, and heterogeneity in the subsurface of the BDP: FSS 1 (least variable) < FSS 2 < FSS 3 (most variable) (e.g., Hadley et al. 2006).

MODERN BARAM DELTA PROVINCE DEPOSITIONAL SYSTEM

Geomorphology

The Modern BDP consists of three distinct, laterally adjacent depositional systems: (1) an open-coastline system comprising a lobate (c. 20 km by 25 km) wave-dominated shelf delta (Baram River delta), and a more laterally extensive (c. 80–100 km long) flanking strandplain that is cut by several smaller rivers (Fig. 11); and (2) a drowned coastal embayment (Brunei Bay; c. 35 km by 50 km) with multiple, mixed-energy bayhead deltas (Fig. 11). Numerous rivers supply sediment to both depositional systems (Figs. 1B, 11), which results in significant along-strike variability in coastal morphology. The 200-km-long, multi-sourced, open shoreline is fed by nine rivers, of which the Baram River has the largest drainage-basin area (19,200 km²) (Figs. 1B, 11) (Mathew et al. 2016a; Mathew et al. 2016b; Menier et al. 2017). Each river forms wave-modified mouth bars that merge into several laterally connected delta lobes and flanking strandplains (Figs. 11, 12). Variations in sediment supply result from a combination of river-mouth bypassing and net transport of sediment alongshore, mainly towards the southwest during the dominant northeast monsoon (Sandal 1996). The interaction of these processes causes coeval shoreline progradation and retreat, mainly on a 3–10 km length-scale and at rates of generally < 1 to c. 5 m/yr along the full (80–100 km long) flanking strandplain (Ahmadi et al. 2011; Collins et al. 2017). However, the significantly larger drainage-basin area of the Baram River, with its consequent higher sediment supply rate, results in several tens of meters per year (up to 78 m/yr) of progradation for the Baram delta mouth bar (Ahmadi et al. 2011). Brunei Bay is fed by eight rivers, spaced 5–25 km apart, with a combined drainage basin area of c. 32,000 km², which exceeds that of the Baram River (Figs. 1B, 11). The rivers feed a series of bayhead deltas, each with a different delta-front morphology (Fig. 13), which reflects the variable interaction between fluvial and basinal (waves and tides) processes. Hence, the Modern BDP clastic

coastal depositional system is characterized by a mixed-process regime that varies according to (1) larger-scale accommodation versus sediment supply (A/S) conditions, and (2) smaller-scale river-mouth-flanking shoreline interactions.

The open coastline is a multi-sourced, “storm-flood”-dominated depositional system, combining simultaneous river floods and storm waves in a monsoon-driven climate (Collins et al. 2017). These mixed processes cause yearly–decadal changes in river-mouth and coastal morphology, seen for instance in the Niah River of the western BDP (Fig. 12). By 2007, a > 1-km-long, alongshore-accreting spit had caused northeast displacement of the river mouth and associated delta (Fig. 12A, B). By 2013, the river had avulsed c. 500 m upstream and fluvio-tidal bars had formed from the eroded spit in the relocated river mouth; infill of the abandoned river mouth by alongshore accretion formed a muddy lagoon and associated tidal inlets (Fig. 12C, D). Similar river-mouth processes and time-scale changes have been noted elsewhere along this laterally extensive flanking strandplain system (e.g., the Seria river mouth in Brunei; Collins et al., 2017).

Brunei Bay is a large (c. 1500 km²) structural embayment, controlled by deep-seated faults (Cullen 2010a), with a range of depositional sub-environments (Figs. 13, 14). These are interpreted to be closely analogous to interpreted Miocene facies successions, particularly those that contain organic-rich, mangrove-dominated mudstone facies; extensive mangrove swamps dominate the intertidal zone that fringes Brunei Bay (Figs. 13, 14). The bay is presently receiving fluvial sediment from five active rivers (from northeast to southwest): Padas, Mangalon, Lawas, Trusan, and Limbang rivers, each containing its own and very distinct bayhead delta, with variable delta-front morphology (Fig. 13A, B). There are many other river mouths that provide negligible fluvial sediment to the bay either because they have been abandoned, mainly through structurally induced river capture, and are now estuaries (e.g., Klias and Brunei rivers, among others), or are short rivers with small

drainage-basin areas (e.g., Temburong River). The wide mouth of the bay comprises a tectonic barrier to the northeast (Klias Peninsula) and a laterally accreting spit (Muara Spit) to the southwest (Fig. 13A, B). The latter receives sand supplied from the Baram delta that is transported alongshore towards the northeast (Fig. 11). Coastal geomorphology in the bay is extremely variable and is determined by (1) the relative interaction of fluvial, wave and tidal processes, (2) the rate of fluvial sediment supply, and (3) the rate of tectonically-induced subsidence.

The northern and Inner Brunei Bay areas are low wave-energy and tide-dominated (Figs. 13A, 14). Extensive networks of fluvio-tidal channels (FS 7) are flanked by mangrove swamps (FS 9). The Padas and Limbang rivers form tide-dominated bayhead deltas containing active river mouths with mangrove-vegetated tidal bars (FS 3) and cut banks (FS 7), while the Klias river mouth forms a relatively inactive estuary with minimal present-day fluvial sediment supply (FS 8–FS 9) (Figs. 13, 14). The Padas and Limbang rivers are building tide-dominated deltas with funnel-shaped geomorphologies (Figs. 13, 14). The wave-affected eastern shoreline comprises mixed-process deltas and flanking strandplains (FS 2) (Fig. 13). The Trusan delta is a river-dominated, wave- and tide-influenced bayhead delta (FS 2 or FS 4) characterized by a lobate geometry and multiple, variably active distributary channels and associated levees and lobes (Figs. 13, 14) (Lambiase et al. 2003). Waves rework mouth bars and levees in basinward positions, where swash bars develop. Deeper (> c. 5–10 m water depth) regions of the embayment are brackish water and likely to be silt- to clay-dominated with infrequent centimeter-scale, sharp-based sandstone beds deposited during storm floods (FS 8) (Abdul Razak 2001).

Sedimentology

Sediment vibracores in the western Brunei Bay share close similarities with strata of the Belait Formation (Figs. 14, 15). In the Limbang River delta, distributary fluvio-tidal channel

sediment comprises sparsely bioturbated, mud-dominated heterolithics with centimeter-scale stratification and minor organic carbon (Fig. 15A). Mouth-bar sediments are thinly stratified (millimeter- to centimeter-scale), muddy heterolithics with common organic debris and a moderate indistinct bioturbation (BI 3–4). The latter is occasionally dominated by small and simple horizontal burrows, including *Planolites* and *Terebellina* (Fig. 15B). The sediment cores in the fluvio-tidal channel and mouth bar resemble F4b in FS 3 and FS 5–FS 7, which are interpreted as deposits of tide-dominated deltas and tide-influenced channels, respectively (Tables 1 and 2). Subtidal mudflat sediment comprises mud and muddy sand with abundant organic debris, minor simple and indistinct bioturbation, and occasional millimeter- to centimeter-scale sand layers and mud clasts (Fig. 15C). Abandoned-tidal-channel sediment is predominantly laminated mudstone with common organic debris and laminae, and occasional mollusk shells and shell fragments (Fig. 15D). Sediment cores in the mudflat and abandoned tidal channel are similar to F2 and F3 in FS 8, which is interpreted to record tidal embayment deposition (Tables 1 and 2).

In the Trusan delta, sediment in distributary-fluvial-channels is dominated by centimeter- to decimeter-scale beds of planar laminated to cross-stratified, very fine- to fine-grained sand with minor mud clasts. Interbedded muddy to sandy heterolithics contain common organic debris and occasional bioturbation, typically consisting of simple subvertical burrows (Fig. 15E). Active-channel-lobe sediment comprises decimeter-scale interbeds of cross-bedded sand and laminated mudstones with common organic-carbon debris and an impoverished ichnofauna comprising occasional sand-filled *Thalassinoidea* burrows (Fig. 15F). Active-fluvial-channel and levee sediments in the Trusan delta are similar to facies in interpreted river-dominated channels (FS 5–FS 6) (Tables 1 and 2). Mouth-bar sediment is dominated by planar-laminated to cross-bedded, very fine- to fine-grained sand with drapes, laminae, and clasts of mud, and common organic-carbon debris, including lags (Fig. 15G). This closely

resembles F8 and F9 in the upper parts of mixed-energy bars and/or deltas (FS 2) but also in fluvio-tidal channels (FS 6–FS 7) (Tables 1 and 2). Delta-front facies consist of sandy to muddy heterolithics and muddy sandstone with sharp-based, centimeter-scale sand layers and moderate bioturbation (BI 2–3), including *Ophiomorpha* (Fig. 15H). This is similar to facies in interpreted delta-front and/or distal-lower-shoreface units in FS 1 and FS 2 (Tables 1 and 2). However, the lack of decimeter-scale sandstone beds may reflect spatial and/or temporal sampling bias. Interdistributary facies comprise muddy heterolithics with millimeter- to centimeter-scale lenticular to wavy bedding, common organic debris, and sporadic bioturbation, which is similar to both interpreted tidal-embayment facies (FS 8) and mixed-energy bars and/or deltas (FS 1–FS 2) (Tables 1 and 2).

Modern and ancient sandstone deposits in the BDP are dominated by very fine- to fine-grained sandstone (Figs. 8, 16) (Atkinson et al. 1986; Lambiase et al. 2002; Lambiase et al. 2003; Collins et al. 2017). Similarly, the median sand-size fraction of sediment on the present-day shelf and in Brunei Bay is very fine- and fine-grained (Fig. 16A), with subordinate medium- and coarse-grained sand (Fig. 16B) (Sandal 1996). However, the present distribution of shelf sand across the eastern BDP, apart from the present-day Baram river mouth, is largely a relic of sand deposition during the Pleistocene lowstand (Sandal 1996). The paleo–Limbang River was probably responsible for the large, sand-rich delta lobe to the northeast of the Modern Baram delta, which was abandoned following the Holocene transgression (Fig. 16). Subsequently, the Limbang River has been abruptly diverted, probably due to tectonics, into its present position in Inner Brunei Bay (Fig. 16).

DISCUSSION

Depositional Model for the Miocene–Modern Baram Delta Province

The Middle Miocene Belait Formation records deposition in an array of mixed-process shoreline environments, covering shelfal to embayment settings (c. 10–100 m, or inner neritic, water depths) (Fig. 17).

Facies succession set 1 records deposition along an open, storm-dominated deltaic shoreline (Fig 17A). Unfortunately, there are no cores from equivalent present-day environments in the BDP. However, based on present-day coastal geomorphology and measured sedimentary processes (Sandal 1996; Ahmadi et al. 2011), FSS 1 is inferred to be directly analogous to sediments accumulating along the multi-sourced, open coastline in the present-day BDP (Fig. 11). By analogy, this probably comprised a wave-dominated delta(s) and flanking strandplain depositional system (Fig. 17A, B). The resulting sandier-upward units preserve episodes of high rates of sediment transport and deposition during low-frequency-high-magnitude storm floods, when storm-wave energy and fluvial discharge were simultaneously elevated (Bhattacharya 2005; Collins et al. 2017). Multiple river delta lobes merge laterally due to strong alongshore fairweather and storm reworking, forming a laterally connected, sheet-like complex of delta lobes and flanking strandplains (Figs. 11, 17A) (Hadley et al. 2006). As the number of fluvial entry points increases, the difference in relative sediment supply decreases and the shoreline assumes a more linear, elongate, strandplain-style geometry (Fig. 17A) (Collins et al. 2017). Consequently, interdistributary regions are less protected from waves and relatively tide-influenced depositional elements are restricted to narrow (sub-kilometer) channels (FS 6–FS 7), bars and/or deltas (FS 3) and embayments (FS 8) that form a subordinate component of the preserved stratigraphic record. However, delta-lobe switching, due to autogenic and/or allogenic processes (Stouthamer and Berendsen 2007), also alters shoreline sediment supply, geomorphology, and, potentially, depositional processes (Fig.

17A, B). In wave-dominated systems, such as the open coastline in the Miocene–Present BDP, waves and storms suppress delta-lobe and distributary-channel avulsion (Swenson 2005). However, active tectonic deformation along the northwest Borneo margin has caused drainage-basin reorganization and delta switching (Mathew et al. 2016a; Mathew et al. 2016b; Menier et al. 2017). This would have increased fluvial influence and sediment supply in some drainage basins, causing shoreline progradation. In contrast, adjacent shorelines fed by less active drainage basins would have experienced diminished sediment supply and relatively increased wave, tide, and storm reworking. Compaction above thick (100s–1000s m), undercompacted prodelta mud would have further enhanced local transgression, including the possible formation of spits and barrier-island systems (Fig. 17B) (e.g., Penland et al. 1988). The spatio-temporal change in depositional environments will be recorded as vertical changes in facies successions, but incomplete preservation could result from: (1) wave, storm, and fluvial reworking associated with shallowing during progradation, including lateral channel migration; and (2) erosion associated with transgression and wave ravinement, principally due to the landward movement of fairweather and storm wave base (e.g., Hampson and Storms 2003; Nienhuis et al. 2013).

Facies succession set 2 records deposition along mixed-process deltaic shorelines subject to wave, fluvial, and tidal influence (Fig. 17C). The increased preservation of combined-flow-rippled heterolithics relative to FSS 1 may reflect a combination of: (1) decreased reworking by peak storm floods, due to lower-frequency and/or lower magnitude events, (2) increased sedimentation rate during higher-frequency-lower-magnitude storm floods, due to increased fluvial influence and/or frequency, and (3) increased rate of accommodation creation, facilitating increased sedimentation and preservation (e.g., Wheatcroft and Drake 2003; Tamura and Masuda 2005). Therefore, FSS 2 may reflect open shoreline–shelf deposition, axial to a river distributary channel, on a high-accommodation, supply-dominated shelf (e.g.,

Swift and Thorne 1991; Reading and Collinson 1996). Alternatively, FSS 2 could also have formed in a relatively low-wave-energy embayment, which would be analogous to the mixed-process, river-dominated Trusan delta in Brunei Bay (Figs. 13, 14, 15E–I) (e.g., Abdul Razak 2001; Lambiase et al. 2003). The decreased thickness of FS 2 in FSS 2 compared to FS 1 in FSS 1 suggests a lower A/S ratio (e.g., Ainsworth et al. 2011), but this is inconsistent with enhanced preservation of higher-frequency-lower-magnitude event deposits. Alternatively, the decrease in FS 2 thickness could reflect an increase in the number and avulsion frequency of distributary channels and delta lobes (Fig. 17C). This would be consistent with (1) higher fluvial power relative to waves (Swenson 2005; Geleynse et al. 2011), (2) higher sedimentation rate (e.g., Bhattacharya and Tye 2004), and/or (3) more frequent allogenic changes (tectonics, eustatic sea level, etc.) (e.g., Hampson 2016). Drainage-basin switching could have created significant spatio-temporal variations in alongshore depositional processes and environments (Fig. 17D), which is consistent with the close stratigraphic association of FSS 2 and the more tide-dominated FSS 3 (Figs. 8C, 10A–C).

The aggradational stacking patterns of both FSS 1 and FSS 2 suggests (1) high rates of sediment supply and accommodation creation, and (2) subordinate fluvio-tidal depositional elements (FS 3–FS 9) (Fig. 6). The lack of preserved lower-coastal-plain deposits, most notably *in situ* coals and soils with mangrove material (FS 9) at the tops of the individual parasequences, probably reflects a combination of (1) transgressive erosion by wave and tidal ravinement, which can be effective even when the shoreline trajectory is strongly positive (Li et al. 2011), and (2) rapid abandonment and drowning during delta or delta lobe switching, which limits the time available to establish extensive vegetation.

Facies succession set 3 represents deposition under increased tide influence and decreased wave and fluvial influence, suggesting a relatively embayed shoreline setting (e.g., present-day Brunei Bay; Figs. 11, 13, 17). In coastal embayments, the absolute strength of tides may

increase due to convergence effects (e.g., Allen 1997) but, equally importantly, the relative strength of tidal currents is likely to be higher because of increased protection from wave and storm currents and flows (e.g., Davis and Hayes 1984; Plink-Björklund 2012). Mangrove mudstones (FS 9) are consistent with tide-dominated deposition under relatively low-wave-energy conditions (Wolanski et al. 1992); present-day mangroves are most prevalent on the fringes of low-wave-energy embayments and abandoned fluvial–tidal channels in humid-tropical delta systems (e.g., Mekong and Ganges-Brahmaputra deltas) (e.g., Woodroffe et al. 2016).

Controls on Grain Size and Sediment Supply

The Middle Miocene of the BDP is dominated by very fine- to fine-grained sandstones, with only local exceptions that mainly comprise thin channel lags (e.g., Fig. 10D, E). However, the relatively short (c. 200–400 km) and high-gradient ($0.3\text{--}3.5^\circ$, averaging $1.5\text{--}2.5^\circ$) rivers (Fig. 1B) would decrease attrition time and increase hydraulic energy, favoring transport and delivery of coarser grains to the shoreline. Only the outcropping Liang Formation contains abundant conglomerate and pebbly sandstone, which was deposited in Plio-Pleistocene braided rivers (Cullen 2010a). There is little quantitative information on sediment grain size in rivers supplying the BDP coastline (Sandal 1996; Abdul Razak 2001). The predominance of very fine- to fine-grained sand reflects several factors: (1) the hinterland rocks are mainly the Oligocene West Crocker Formation and the Middle Oligocene–Early Miocene Meligan Formation, which contain abundant compositionally and texturally mature, fine- to coarse-grained sandstone and thick intercalated mudstones (Sandal 1996; Moss 1998; Hutchison 2005; Jackson et al. 2009; van Hattum et al. 2013), (2) an ever-wet, humid-tropical climate results in deep tropical weathering that produces finer-grained sediment, (3) within the present-day Limbang, Temburong, and Trusan rivers, coarser sediment (including pebbles and cobbles) is trapped in upstream to midstream bars and channels (Abdul Razak 2001), (4)

sand grains may undergo attrition during transfer in channels and within bars, and (5) dense tropical rainforest vegetation and soil, which was fully established by the Miocene (Heaney 1991), are likely to trap more sediment. However, up to 9–12 km of Middle Miocene–Recent sedimentation also suggests a high rate and efficient supply of sediment to the shoreline, which is likely to reflect three main factors: (1) exhumation of a previously higher-elevation hinterland (Hall and Nichols 2002; Morley and Back 2008) with larger areas above the tree line, (2) climate-driven variations in the size of the area above the tree line (Verstappen 1975), and (3) efficient transfer of sediment through the short rivers during infrequent (1000 year), large-magnitude, high-intensity, localized storms (“storm flood” events) (Collins et al. 2017).

Formation of Tide-Dominated Embayments: Regional versus Local Transgression

Tide-dominated embayments are mostly interpreted to form during transgression (Fig. 17E) (Yoshida et al. 2004; Sixsmith et al. 2008), especially by flooding of incised valleys (e.g., Van Wagoner 1991; Dalrymple et al. 1992) or the abandonment of distributary channels (Oomkens 1974; Allen and Chambers 1998). Holocene flooding of the Baram River valley formed a tide-dominated and mangrove-vegetated estuary (Caline and Huong 1992), but tide-dominated embayments may also form by local transgression along net-regressive coastlines (Fig. 17A–D). For instance, the Holocene evolution of the river-dominated Mississippi River delta indicates that autocompaction and marine reworking of abandoned delta lobes (for a distributive delta plain) or deltas (along multi-sourced deltaic shorelines) causes shoreline retreat, barrier-lagoon and bay formation, and conversion of former distributary channels to sediment-starved estuaries (e.g., Frazier 1967; Penland et al. 1985; Penland et al. 1988; Roberts and Coleman 1996). The Mississippi River delta is fed by a single large river (c. 4,000 km) that supplies a distributive network with multiple, river-dominated delta lobes. In contrast, the Miocene–Present BDP is a mixed-process system, with multiple, short (c. 200–

400 km) rivers feeding coalesced delta lobes that merge laterally via flanking strandplains (Figs. 1B, 11, 17) (Ahmadi et al. 2011; Collins et al. 2017). Transgressive sub-environments (FSS 3) could have formed (1) between river deltas (FSS 1 or FSS 2), (2) along abandoned river mouths, and/or (3) in areas of tectonically-enhanced subsidence (e.g. caused by gravitational loading and/or reactivation of basement-linked faults). The most likely controlling mechanism in the Miocene–Modern is tectonically driven switching of drainage basins, which causes major changes in the rate and volume of sediment flux (Mathew et al. 2016a; Mathew et al. 2016b; Menier et al. 2017).

Tectonically controlled embayments (e.g., Brunei Bay; Fig. 13) may form in a shoreline–shelf system at any stage of a RSL cycle (Fig. 17F). If the embayment is smaller than the shoreline–shelf system, contemporaneous embayment and open-coastline depositional systems are formed, which may individually comprise several coeval and time-varying sub-environments governed by various depositional processes (Fig. 17F). If sediment supply keeps pace with subsidence, the high rate of burial in tectonic embayments increases the preservation potential of sediments. In the BDP, the spacing between major, basement-linked and sub-basin bounding faults that were variably active in the Middle Miocene–Pliocene is approximately 10–30 km (Sandal 1996; Morley et al. 2003). Therefore, temporal variations in the rate of fault movement could have segmented the 100-km-scale shoreline–shelf system into coeval open and embayed shoreline–shelf systems (Cullen 2010a).

Comparison with Mixed-Process Ancient Stratigraphy

Shoreline–shelf deposits displaying evidence of mixed-process, tide- and wave-influenced regimes have been recognized in other ancient systems. The Early Miocene Nyalau Formation and c. Middle–Late Miocene Balingian Formation in the Balingian Province, Sarawak, comprises a range of facies successions very similar to that of the Belait Formation, including interpreted deposits of mixed-process deltas, fluvio-tidal channels, and tide-

dominated embayments and deltas (Amir Hassan et al. 2013; Amir Hassan et al. 2016; Murtaza et al. 2018). However, there is an increased preservation of *in situ* organic-rich mangrove facies (coal seams), tidal bar and/or delta successions, and fluvio-tidal channels, which suggests stronger tidal and fluvial processes (Amir Hassan et al. 2013; Amir Hassan et al. 2016; Murtaza et al. 2018).

Late Oligocene–Early Miocene strata in the Eastern Venezuela Basins, and genetically linked Pliocene successions in the adjacent Columbus Basin (Mayaro Formation), are also interpreted to record deposition in contemporaneous storm-dominated deltas, wave-dominated flanking strandplains, and more tidally influenced interdistributary bays under a tropical-humid climate (Buatois et al. 2008; Buatois et al. 2012; Bowman and Johnson 2014; Chen et al. 2014). However, contemporaneous deposition in river-dominated deltas along open coastlines is also interpreted, unlike in the Miocene–Modern BDP.

The depositional model of the Late Cretaceous lower Sego Sandstone of the Western Interior Seaway, North America, shares similarities with the interpreted depositional model of the Miocene–Modern BDP, including (1) a wave-dominated delta front, (2) active and inactive regions of the delta plain, and (3) a lack of preserved fluvial-dominated mouth bars (Legler et al. 2014; van Cappelle et al. 2016). However, differences include (1) a lower number of feeder rivers, (2) a tide-dominated lower delta plain, and (3) wide-mouthed distributaries.

The Middle Jurassic Lajas Formation of the Neuquén Basin is attributed to deposition in two contrasting settings (1) a mixed-energy, wave- and tide-dominated, river-influenced shoreline–shelf system (Rossi and Steel 2016), and (2) fluvial–tidal channels and fluvial-dominated, tide-influenced crevasse-sub-deltas in a river-dominated lower delta plain (Gugliotta et al. 2015; Gugliotta et al. 2016a; Gugliotta et al. 2016b). These two models are compatible if the river-dominated and tide-influenced delta plain was formed in an

abandoned region of the larger-scale, mixed-energy system. Similarities between the mixed-energy-delta model and the Miocene–Modern BDP include (1) a mixed wave-fluvial lower delta plain, (2) wave-dominated flanking strandplain and offshore deposits, and (3) lateral variations in process dominance (Rossi and Steel 2016). However, differences include (1) a single-sourced and distributive delta system, (2) a tide-dominated delta front, and (3) coarser-grained and sand-rich facies. The model of a river-dominated lower delta plain includes similar mixed fluvial–tidal channels and deltas to low-wave-energy embayments in the Miocene–Modern BDP but is incompatible with the wave-dominated open-coastline system.

In the Late Cretaceous Horseshoe Canyon Formation, delta-front and/or shoreface facies, which are otherwise very similar to FS 1 in the Belait Formation, are interpreted to record wave-dominated and tide-influenced deposition because of frequent and often double mud and carbonaceous drapes in swaly cross-stratified sandstone (Vakarelov et al. 2012).

However, without statistical and harmonic analysis of the drapes (e.g., Kvale et al. 1989; Kvale 2012), the degree of tidal influence is inconclusive, despite the more conclusive interpretation of tidal deposition in directly overlying stratigraphic units (Ainsworth et al. 2015; Ainsworth et al. 2017).

Comparison with Mixed-Process Holocene–Modern Systems

Early shoreline classifications emphasized wave-, tide- and river-dominated end members (Coleman and Wright 1975; Galloway 1975). However, in reality, all modern shorelines along oceans and seas show varying degrees of mixed influence because tides and weather systems operate globally. This recognition of mixed processes underpins the move towards a higher-resolution ternary process diagram (Ainsworth et al. 2011), which is consistent with the spatial–temporal variations in sedimentary processes in Holocene–Modern shoreline–shelf systems.

Radiocarbon-dated sediment cores in the Holocene–Modern Mekong delta suggest that deposition before c. 3 ka occurred in a tide-dominated delta within a low-wave-energy, mangrove-vegetated coastal embayment (e.g., Ta et al. 2002; Tanabe et al. 2003; Ta et al. 2005). Similar tide-dominated deposition occurred in low-wave-energy embayments in the Miocene–Modern BDP (Caline and Huong 1992). Since c. 3 ka, deposition in the Mekong delta is interpreted to have occurred predominantly in a mixed tide- and wave-dominated, open-coastline delta (Tanabe et al. 2003; Ta et al. 2005). Tidal dominance in the interpreted delta front contrasts with the open-coastline system in the Miocene–Modern BDP, but similarities include the wave-dominated, tide-influenced lower delta plain and decreased abundance of mangrove vegetation.

The present-day funnel-shaped Fly River delta is tide-dominated (Galloway 1975; Dalrymple et al. 2003); however, unambiguous indicators of tidal processes are rare in heterolithic sediment from channels, bars, and the delta front (Dalrymple et al. 2003). This is remarkably similar to heterolithic facies in the Belait Formation. However, the statistical signal of tidality may be obscured by erosion during spring tides, mud-layer amalgamation, anomalously thick fluid-mud deposits, and/or formation of sporadic couplets during the subordinate tide (Dalrymple et al. 2003). Sediments in the present-day Fly River delta are very similar to interpreted tide-dominated embayment successions (FSS 3) in the Belait Formation, but are rarely preserved in interpreted open-coastline successions (FSS 1 and FSS 2). Wave influence on the Fly River delta is low, with a median 1.8 m significant wave height during the southeast monsoon (Thom and Wright 1983), and preserved indicators of wave influence are minimal (Dalrymple et al. 2003). The median wave height along the Modern BDP open coastline is similarly low (< 1 m), although waves can exceed heights of 3 m during the north-east monsoon (Sandal 1996). However, the Middle Miocene Belait Formation preserves significant evidence of storm-dominated, open-coastline deposition, which

suggests: (1) the storm-wave climate was stronger in the Middle Miocene (Collins et al. 2017); and/or (2) the highest-magnitude-lowest-frequency storm events, which are not recorded in the short-timespan (1984–1994) wave data, are disproportionately preserved. The Fly River delta cores are not age dated and may not record deposition during high-magnitude–low-frequency storms, and/or sedimentation during these events may be different than in the BDP due to diminished sand supply to the shoreline (Dalrymple et al. 2003).

Selecting a Modern Analogue

Modern analogues for ancient shoreline–shelf depositional systems should be selected based on the consistency of several geological criteria, of which the principal criteria are (1) tectonic setting, which influences the physiography of source-to-sink systems (Sømme et al. 2009) and rate of accommodation creation, (2) climatic setting, which influences precipitation, weathering, fluvial discharge and sediment supply rates, wave and storm climate, and vegetation type, and (3) whether the shoreline is depositional or erosional (Nyberg and Howell 2016).

Interpretation of process dominance in modern shoreline–shelf systems continues to rely heavily on plan-view geomorphology (Coleman and Wright 1975; Galloway 1975; Vakarelov and Ainsworth 2011; Nanson et al. 2013). The absolute strength of wave height, tidal range, and fluvial discharge are common quantitative data, but they are limited in their use for determining process dominance between modern systems without underlying assumptions regarding shoreline morphology (Nyberg and Howell 2016). For example, tidal range versus wave height differentiates wave- versus tide-dominated barrier morphologies (Hayes 1979), but barrier morphologies in mixed-energy systems are statistically indistinct (Mulhern et al. 2017).

Additional criteria for selecting modern analogues may include (1) transgressive versus regressive systems, (2) linear-lobate versus funnel-shaped shoreline morphology, (3) single- versus multi-sourced fluvial system, (4) distributive versus non-distributive fluvial system, and (5) drainage basin area.

The Miocene–Modern BDP provides a rare case study where ancient stratigraphy can be compared with the very similar, and geographically adjacent, equivalent modern system. Other mixed wave- and tide-influenced deltaic systems are less complete analogs for the Middle Miocene Belait Formation. For example, the Orinoco, Mekong, Niger, and Zambezi deltas all occur in tropical latitudes but are distributive, formed by significantly larger rivers, and variably occur in passive-margin settings (Oomkens 1974; Ta et al. 2002; Warne et al. 2002; Aslan et al. 2003; Tamura et al. 2012). In contrast, the Copper, Olenyok, and West Lena deltas are formed under permafrost conditions (Galloway 1976). Thorough comparison with one very similar modern analogue permits more defensible interpretations of process dominance, planform geomorphology, and the geological controls (allogenic and autogenic) on ancient deposition.

Comparing Modern Shoreline–Shelf Systems with Ancient Stratigraphy

The key condition for preservation of shoreline–shelf environments in the stratigraphic record is the rate of burial exceeding the rate of erosion. In shoreline–shelf environments, there are twelve erosional processes (“sedimentation-rate scales”) with repeat times spanning 14 orders of magnitude (Fig. 18A) (Miall 1991; Bailey and Smith 2010; Miall 2015). Sub-yearly processes, which include fairweather waves, non-flood fluvial discharge, tides (daily and spring–neap) and ocean currents (processes 1–4, Fig. 18), are unlikely to cause significant and widespread erosion because these processes (1) are associated with the highest instantaneous rates of sedimentation (Fig. 18A) (Miall 2015), and (2) operate across a relatively narrow depth range and small area (Fig. 18B, C); fairweather waves occur above

fairweather wave base, tides occur between neap and spring tide levels and non-flood fluvial discharge is most commonly hypopycnal (e.g., Lamb and Mohrig 2009). In addition, ocean currents, such as internal waves and tides, more typically influence outer shelf–slope environments (e.g., Pomar et al. 2012). Yearly to thousand-year processes potentially cause more erosion over a larger area and depth range, and include (1) seasonal to 1000-year river floods, (2) storms and combined “storm floods” (Collins et al. 2017), and (3) autogenic geomorphic processes, such as channel and delta lobe switching (processes 5–7, Fig. 18). Lower-frequency-higher-magnitude storms and floods typically form thicker beds with a higher preservation potential than those formed during higher-frequency-lower-magnitude processes (e.g., Dott 1983; Thorne et al. 1991). In contrast, higher-magnitude-lower-frequency storms, floods, and autogenic geomorphic processes also influence stratigraphic preservation due to the reorganization of deltaic distributary channels and lobes, incision associated with channel avulsion, erosion of the adjacent delta front and flanking strandplain, and erosion during relative transgression of abandoned channels and lobes (e.g., Storms and Hampson 2005). However, these changes are only likely to occur on the scale of a single feeder channel and delta (1–10 km in the BDP) (Figs. 17A–D, 18B, C) and laterally adjacent environments of varying process may be unaffected.

On a 10^4 – 10^7 year timescale, climatic variations and tectonics (processes 8–12, Fig. 18) may cause changes in river discharge and sediment supply, drainage-basin reorganization (principally tectonic uplift versus subsidence) and RSL changes, which lead to larger-scale (100s km) changes to shoreline–shelf deposition (Figs. 17, 18C, D). Geomorphic changes, which include net transgression (during system-wide RSL rise), initiation of new prograding deltas, and local transgression of abandoned shoreline areas may all be associated with significant erosion. Multi-sourced deltaic shorelines in active tectonic settings, such as the BDP, will be particularly prone to tectonically controlled drainage-basin reorganization. The

relative impact of climate-driven eustatic sea-level changes versus tectonically driven subsidence and uplift depends on the rate of each process. In the BDP, during the Late Miocene–Pliocene, both the average rate of hinterland uplift and basin subsidence were approximately 500 mm/kyr (Sandal 1996; Morley and Back 2008), which would have greatly exceeded the long-term rate of eustatic sea-level change during this period (c. 1 mm/kyr; Miller et al. 2005). However, short-term (10^3 yr) glacio-eustatic sea-level fluctuations may have been up to 1000 mm/kyr, equal to the short-term (10^3 yr) rates of tectonic movement on sub-basin-bounding faults (e.g., Sandal 1996; Goldsworthy and Jackson 2001).

CONCLUSIONS

The BDP source-to-sink system has operated for the past c. 15 Myr in a relatively consistent tectonic (active foreland margin) and climatic setting (humid-tropical, ever-wet, and monsoon-influenced). A comparison of facies and stratigraphic analysis of Miocene strata and process-based geomorphological and sedimentological investigations of present-day environments in the BDP concludes that the present-day mixed-process depositional system offers a very close analogue to the surface and subsurface Miocene–Pliocene successions, and *vice-versa*.

The Middle Miocene Belait Formation in the Berakas Syncline (eastern BDP) accumulated in a range of shoreline–shelf environments under varying wave, fluvial, and tidal conditions. Three main facies succession sets (parasequence sets) comprise distinct groups of facies successions (parasequences) and define distinctive reservoir-scale intervals:

- (1) Wave-dominated deltas and/or flanking strandplains (FSS 1) comprise aggradationally stacked, upward-sanding parasequences (10–50 m thick) dominated by sharp-based sandstone beds showing swaly cross-stratification and abundant, decimeter- to meter-scale gutter casts (FS 1). Deposition occurred during large-

magnitude storm floods, which are characterized by simultaneously high storm-wave energy and storm-enhanced fluvial discharge (“storm floods”). Similar deposition is inferred along the multi-sourced, open deltaic coastline of the present-day BDP.

- (2) Mixed-process deltas and/or flanking strandplains (FSS 2) comprise aggradationally-stacked, upward-sanding parasequences containing interbedded swaley cross-stratified sandstone and combined-flow-rippled heterolithics (FS 2). Deposition occurred under fluctuating sediment supply and energy, during storm floods of lower frequency and magnitude and higher fluvial influence. Present-day sediment cores from the BDP indicate that similar deposition occurs along wave-affected, multi-sourced, embayed deltaic coastlines (e.g., Trusan delta, Brunei Bay).
- (3) Tide-dominated, wave- and river-influenced, coastal embayment successions (FSS 3) comprise a range of facies successions and display the greatest reservoir heterogeneity: (i) variably heterolithic and bioturbated (BI 0–5) mudstones (FS 8), (ii) carbonaceous mangrove mudstones (FS 9), (iii) sharp-based, fining-upwards, fluvio-tidal channels (FS 6–FS 7), (iv) upward-sanding, heterolithic, tidal bars (FS 3), and (v) mixed-process deltas and/or flanking strandplains (FS 2). Present-day sediment cores from the BDP indicate that similar depositional environments occur in Brunei Bay (e.g., Limbang and Padas deltas).

Mixed-process deposition is consistent with the geological characteristics of the mid-Miocene to present-day BDP source-to-sink system:

- (1) High storm-wave reworking reflects deposition along monsoon-influenced coastlines open to the South China Sea.
- (2) A highly effective and efficient fluvial sediment-supply system, due to (i) an actively uplifting, high-elevation (c. 2–4 km) hinterland, comprising erodible mudstone and

sandstone, (ii) a narrow and steep coastal plain (< 100 km; c. 1°) and shelf (< 100 km; c. 0.1°), and (iii) multiple small (10^2 – 10^5 km²) drainage basins.

- (3) High accommodation due to delta tectonics and reactivation of recently formed (Oligocene) basement-linked faults.
 - (4) Formation of low-wave-energy, tide-dominated embayments due to (i) marine reworking and autocompaction of abandoned delta lobes and deltas, (ii) flooding of river valleys during eustatic sea-level transgressions, and (iii) subsidence caused by basement-linked faulting.
 - (5) Active tectonic deformation perturbs surface morphology and causes drainage-basin reorganization and variations in sediment supply along shoreline–shelf systems.
- Tectonic forcing has continued to be the major cause of stratigraphic complexity in ancient successions in the BDP, ever since the formation of the source-to-sink system at the start of the Middle Miocene (c. 15 Ma).

ACKNOWLEDGMENTS

This work was funded by a Natural Environment Research Council (NERC) PhD scholarship (D.S.C.; award ref. 1318033). Fieldwork was supported by Shell International Exploration and Production (D.S.C and H.D.J.) and Brunei Shell Petroleum Co. Ltd. (A.R.D.). We also acknowledge support of Brunei Shell Petroleum Co. Ltd. during a four-month placement (D.S.C) and Getech (D.S.C. and P.A.A.). We also thank M. van Cappelle and C.D. Dean for fieldwork assistance and many other geoscientists for stimulating discussions, notably G.J. Hampson, B.K. Levell, D. Gray, S. Large, A. Kassam, T. Goodall, M. Mueller, B. Lehner, and I. De Lugt. This manuscript greatly benefited from the thorough edits of J.B. Southard.

REFERENCES

- ABDUL RAZAK, D., 2001, Brunei Bay, Northwest Borneo: Depositional System: University of Aberdeen, 529 p.
- AHMADI, A., CUMMINGS, P.D., BETTINGTON, S.H., and ROUNDS, F., 2011, Two-dimensional coastal sediment transport modelling of Miri coast, Sarawak: Coasts and Ports 2011: Diverse and Developing: Proceedings of the 20th Australasian Coastal and Ocean Engineering Conference and the 13th Australasian Port and Harbour Conference, p. 1-6.
- AINSWORTH, R.B., VAKARELOV, B.K., and NANSON, R.A., 2011, Dynamic spatial and temporal prediction of changes in depositional processes on clastic shorelines: Toward improved subsurface uncertainty reduction and management: American Association of Petroleum Geologists, Bulletin, v. 95, p. 267-297.
- AINSWORTH, R.B., VAKARELOV, B.K., LEE, C., MACEACHERN, J.A., MONTGOMERY, A.E., RICCI, L.P., and DASHTGARD, S.E., 2015, Architecture and evolution of a regressive, tide-influenced marginal marine succession, Drumheller, Alberta, Canada: Journal of Sedimentary Research, v. 85, p. 596-625.
- AINSWORTH, R.B., VAKARELOV, B.K., MACEACHERN, J.A., RARITY, F., LANE, T.I., and NANSON, R.A., 2017, Anatomy of a Shoreline Regression: Implications for the high-resolution stratigraphic architecture of deltas: Journal of Sedimentary Research, v. 87, p. 425-459.
- ALLEN, G.P., and CHAMBERS, J.L.C., 1998, Sedimentation in the modern and Miocene Mahakam Delta: Jakarta, Indonesian Petroleum Association, 236 p.
- ALLEN, P.A., 1997, Earth Surface Processes: Oxford, U.K., Blackwell Scientific Publications, 404 p.
- AMIR HASSAN, M.H., JOHNSON, H.D., ALLISON, P.A., and ABDULLAH, W.H., 2013, Sedimentology and stratigraphic development of the upper Nyalau Formation (Early Miocene), Sarawak, Malaysia: A mixed wave- and tide-influenced coastal system: Journal of Asian Earth Sciences, v. 76, p. 301-311.
- AMIR HASSAN, M.H., JOHNSON, H.D., ALLISON, P.A., and ABDULLAH, W.H., 2016, Sedimentology and stratigraphic architecture of a Miocene retrogradational, tide-dominated delta system: Balingian Province, offshore Sarawak, Malaysia, *in* Hampson, G.J., Reynolds, A.D., Kostic, B., and Wells, M.R., eds., Sedimentology of Paralic Reservoirs: Recent Advances: Geological Society of London, Special Publication 444, SP444.12, 36 p.
- ARNOTT, R.W.C., 1993, Quasi-planar-laminated sandstone beds of the Lower Cretaceous Bootlegger Member, north-central Montana: evidence of combined-flow sedimentation: Journal of Sedimentary Petrology, v. 63, p. 488-494.
- ASLAN, A., WHITE, W.A., WARNE, A.G., and GUEVARA, E.H., 2003, Holocene evolution of the western Orinoco Delta, Venezuela: Geological Society of America, Bulletin, v. 115, p. 479-498.
- ATKINSON, C.D., GOESTEN, M.J.B.G., SPEKSNEIJDER, A., and VAN DER VLUGT, W., 1986, Storm-generated sandstone in the Miocene Miri Formation, Seria Field, Brunei (NW Borneo), *in* Knight, R.J., and McLean, J.R., eds., Shelf Sands and Sandstones: Canadian Society of Petroleum Geologists, Memoir 11, p. 213-240.
- BAAS, J.H., BEST, J.L., and PEAKALL, J., 2016, Predicting bedforms and primary current stratification in cohesive mixtures of mud and sand: Geological Society of London, Journal, v. 173, p. 12-45.

- BACK, S., TIOE, H.J., THANG, T.X., and MORLEY, C.K., 2005, Stratigraphic development of synkinematic deposits in a large growth-fault system, onshore Brunei Darussalam: Geological Society of London, Journal, v. 162, p. 243-257.
- BAILEY, R.J., and SMITH, D.G., 2010, Thematic set: scaling in stratigraphic data series: implications for practical stratigraphy: First Break, v. 28, p. 57-66.
- BANN, K.L., TYE, S.C., MACEACHERN, J.A., FIELDING, C.R., and JONES, B.G., 2008, Ichnological and sedimentological signatures of mixed wave-and storm-dominated deltaic deposits: examples from the early Permian Sydney Basin, Australia, *in* Hampson, G.J., Steel, R.J., Burgess, P.M., and Dalrymple, R.W., eds., Recent Advances in Models of Siliciclastic Shallow-Marine Stratigraphy: SEPM, Special Publication 90, p. 293-332.
- BHATTACHARYA, J.P., and TYE, R.S., 2004, Searching for modern Ferron analogs and application to subsurface interpretation, *in* Chidsey, T.C.J., Adams, R.D., and Morris, T.H., eds., Regional to Wellbore Analog for Fluvial-Deltaic Reservoir Modeling: The Ferron Sandstone of Utah: American Association of Petroleum Geologists, Studies in Geology 50 p. 39-57.
- BHATTACHARYA, J.P., 2005, Distinguishing shorefaces versus delta fronts in the rock record: American Association of Petroleum Geologists Annual Convention: Calgary, Alberta, Abstract.
- BOWMAN, A.P., and JOHNSON, H.D., 2014, Storm-dominated shelf-edge delta successions in a high accommodation setting: The palaeo-Orinoco Delta (Mayaro Formation), Columbus Basin, South-East Trinidad: Sedimentology, v. 61, p. 792-835.
- BUATOIS, L.A., SANTIAGO, N., PARRA, K., and STEEL, R.J., 2008, Animal-substrate interactions in an Early Miocene wave-dominated tropical delta: Delineating environmental stresses and depositional dynamics (Tacata Field, Eastern Venezuela): Journal of Sedimentary Research, v. 78, p. 458-479.
- BUATOIS, L.A., SANTIAGO, N., HERRERA, M., PLINK-BJÖRKLUND, P., STEEL, R.J., ESPIN, M., and PARRA, K., 2012, Sedimentological and ichnological signatures of changes in wave, river and tidal influence along a Neogene tropical deltaic shoreline: Sedimentology, v. 59, p. 1568-1612.
- CALINE, B., and HUONG, J., 1992, New insight into the recent evolution of the Baram Delta from satellite imagery: Geological Society of Malaysia, Bulletin, v. 32, p. 1-13.
- CATUNEANU, O., 2006, Principles of Sequence Stratigraphy: Amsterdam, Elsevier Science, 386 p.
- CHARVIN, K., HAMPSON, G.J., GALLAGHER, K.L., STORMS, J.E., and LABOURDETTE, R., 2011, Characterization of controls on high-resolution stratigraphic architecture in wave-dominated shoreface-shelf parasequences using inverse numerical modeling: Journal of Sedimentary Research, v. 81, p. 562-578.
- CHEN, S., STEEL, R.J., DIXON, J.F., and OSMAN, A., 2014, Facies and architecture of a tide-dominated segment of the Late Pliocene Orinoco Delta (Morne L'Enfer Formation) SW Trinidad: Marine and Petroleum Geology, v. 57, p. 208-232.
- COLEMAN, J.M., and WRIGHT, L.D., 1975, Modern river deltas: variability of processes and sand bodies, *in* Broussard, M.L., ed., Deltas: Models for Exploration: Houston, Texas, Houston Geological Society, p. 99-149.
- COLLINS, D.S., JOHNSON, H.D., ALLISON, P.A., GUILPAIN, P., and DAMIT, A.R., 2017, Coupled 'storm-flood' depositional model: Application to the Miocene-Modern Baram Delta Province, north-west Borneo: Sedimentology, v. 64, p. 1203-1235.
- CULLEN, A.B., 2010a, The Klias Peninsula and Padas River, NW Borneo: An Example of Drainage Capture in an Active Tropical Foreland Basin, American Association of Petroleum Geologists, Search and Discovery Article #50294.

- CULLEN, A.B., 2010b, Transverse segmentation of the Baram–Balabac Basin, NW Borneo: refining the model of Borneo's tectonic evolution: *Petroleum Geoscience*, v. 16, p. 3-29.
- DALRYMPLE, R.W., ZAITLIN, B.A., and BOYD, R., 1992, Estuarine facies models: conceptual basis and stratigraphic implications: perspective: *Journal of Sedimentary Petrology*, v. 62, p. 1130-1146.
- DALRYMPLE, R.W., BAKER, E.K., HARRIS, P.T., and HUGHES, M.G., 2003, Sedimentology and stratigraphy of a tide-dominated, foreland-basin delta (Fly River, Papua New Guinea), *in* Sidi, F.H., Nummedal, D., Imbert, P., Darman, H., and Posamentier, H.W., eds., *Tropical Deltas of Southeast Asia; Sedimentology, Stratigraphy, and Petroleum Geology: SEPM, Special Publication 76*, p. 147–173.
- DALRYMPLE, R.W., and CHOI, K., 2007, Morphologic and facies trends through the fluvial–marine transition in tide-dominated depositional systems: A schematic framework for environmental and sequence-stratigraphic interpretation: *Earth-Science Reviews*, v. 81, p. 135-174.
- DAVIS, R.A., and HAYES, M.O., 1984, What is a wave-dominated coast?: *Marine Geology*, v. 60, p. 313-329.
- DOTT, R.H., and BOURGEOIS, J., 1982, Hummocky stratification: significance of its variable bedding sequences: *Geological Society of America, Bulletin*, v. 93, p. 663-680.
- DOTT, R.H., 1983, Episodic Sedimentation—How Normal Is Average? How Rare Is Rare? Does It Matter?: *Journal of Sedimentary Petrology*, v. 53, p. 5-23.
- DOUGLAS, I., BIDIN, K., BALAMURUGAN, G., CHAPPELL, N.A., WALSH, R., GREER, T., and SINUN, W., 1999, The role of extreme events in the impacts of selective tropical forestry on erosion during harvesting and recovery phases at Danum Valley, Sabah: *Royal Society (London), Philosophical Transactions, B: Biological Sciences*, v. 354, p. 1749-1761.
- DUMAS, S., ARNOTT, R.W.C., and SOUTHARD, J.B., 2005, Experiments on oscillatory-flow and combined-flow bed forms: Implications for interpreting parts of the shallow-marine sedimentary record: *Journal of Sedimentary Research*, v. 75, p. 501-513.
- DYKES, A.P., 2000, Climatic patterns in a tropical rainforest in Brunei: *The Geographical Journal*, v. 166, p. 63-80.
- FLOOD, Y.S., and HAMPSON, G.J., 2014, Facies and architectural analysis to interpret avulsion style and variability: Upper Cretaceous Blackhawk Formation, Wasatch Plateau, Central Utah, U.S.A: *Journal of Sedimentary Research*, v. 84, p. 743-762.
- FRAZIER, D.E., 1967, Recent deltaic deposits of the Mississippi River: their development and chronology: *Gulf Coast Association of Geological Societies, Transactions*, v. 17, p. 287-315.
- GALLOWAY, W.E., 1975, Process framework for describing the morphologic and stratigraphic evolution of deltaic depositional systems, *in* Broussard, M.L., ed., *Deltas: Models for Exploration: Houston, Texas, Houston Geological Society*, p. 87-98.
- GALLOWAY, W.E., 1976, Sediments and stratigraphic framework of the Copper River fan-delta, Alaska: *Journal of Sedimentary Petrology*, v. 46, p. 726-737.
- GARTRELL, A., TORRES, J., and HOGGMASCALL, N., 2011, A Regional Approach to Understanding Basin Evolution and Play Systematic in Brunei—Unearthing New Opportunities in a Mature Basin: *International Petroleum Technology Conference*.
- GELEYNSE, N., STORMS, J.E.A., WALSTRA, D.-J.R., JAGERS, H.R.A., WANG, Z.B., and STIVE, M.J.F., 2011, Controls on river delta formation: insights from numerical modelling: *Earth and Planetary Science Letters*, v. 302, p. 217-226.

- GINGRAS, M.K., MACEACHERN, J.A., and PEMBERTON, S.G., 1998, A comparative analysis of the ichnology of wave-and river-dominated allomembers of the Upper Cretaceous Dunvegan Formation: *Bulletin of Canadian Petroleum Geology*, v. 46, p. 51-73.
- GOLDSWORTHY, M., and JACKSON, J., 2001, Migration of activity within normal fault systems: examples from the Quaternary of mainland Greece: *Journal of Structural Geology*, v. 23, p. 489-506.
- GOMIS-CARTESIO, L.E., POYATOS-MORÉ, M., FLINT, S.S., HODGSON, D.M., BRUNT, R.L., and WICKENS, H.D., 2016, Anatomy of a mixed-influence shelf edge delta, Karoo Basin, South Africa, *in* Hampson, G.J., Reynolds, A.D., Kostic, B., and Wells, M.R., eds., *Sedimentology of Paralic Reservoirs: Recent Advances: Geological Society of London, Special Publication 444, SP444.5*, 26 p.
- GUGLIOTTA, M., FLINT, S.S., HODGSON, D.M., and VEIGA, G.D., 2015, Stratigraphic record of river-dominated crevasse subdeltas with tidal influence (Lajas Formation, Argentina): *Journal of Sedimentary Research*, v. 85, p. 265-284.
- GUGLIOTTA, M., FLINT, S.S., HODGSON, D.M., and VEIGA, G.D., 2016a, Recognition criteria, characteristics and implications of the fluvial to marine transition zone in ancient deltaic deposits (Lajas Formation, Argentina): *Sedimentology*, v. 63, p. 1971-2001.
- GUGLIOTTA, M., KURCINKA, C.E., DALRYMPLE, R.W., FLINT, S.S., and HODGSON, D.M., 2016b, Decoupling seasonal fluctuations in fluvial discharge from the tidal signature in ancient deltaic deposits: an example from the Neuquén Basin, Argentina: *Geological Society of London, Journal*, v. 173, p. 94-107.
- HADLEY, D.F., AROCHUKWU, E.C., NISHI, K., SARGINSON, M.J., SALLEH, H., and OMAR, M., 2006, Depositional Modelling of Champion Field, Brunei, *Society of Petroleum Engineers Asia Pacific Oil and Gas Conference and Exhibition: Adelaide, Australia, Society of Petroleum Engineers*.
- HALL, R., and NICHOLS, G., 2002, Cenozoic sedimentation and tectonics in Borneo: climatic influences on orogenesis, *in* Jones, S.J., and Frostick, L., eds., *Sediment Flux to Basins: Causes, Controls and Consequences: Geological Society of London, Special Publication 191*, p. 5-22.
- HAMPSON, G.J., and STORMS, J.E.A., 2003, Geomorphological and sequence stratigraphic variability in wave-dominated, shoreface-shelf parasequences: *Sedimentology*, v. 50, p. 667-701.
- HAMPSON, G.J., 2016, Towards a sequence stratigraphic solution set for autogenic processes and allogenic controls: Upper Cretaceous strata, Book Cliffs, Utah, USA: *Geological Society of London, Journal*, v. 173, p. 817-836.
- HAYES, M.O., 1979, Barrier island morphology as a function of tidal and wave regime, *in* Leatherman, S.P., ed., *Barrier Islands: New York, Academic Press*, p. 1-27.
- HEANEY, L.R., 1991, A synopsis of climatic and vegetational change in Southeast Asia: *Climatic Change*, v. 19, p. 53-61.
- HISCOTT, R.N., 2001, Depositional sequences controlled by high rates of sediment supply, sea-level variations, and growth faulting: the Quaternary Baram Delta of northwestern Borneo: *Marine Geology*, v. 175, p. 67-102.
- HOWARD, J.D., and REINECK, H.-E., 1981, Depositional facies of high-energy beach-to-offshore sequence: comparison with low-energy sequence: *American Association of Petroleum Geologists, Bulletin*, v. 65, p. 807-830.
- HUTCHISON, C.S., 2005, *Geology of North-West Borneo: Sarawak, Brunei and Sabah: Amsterdam, Elsevier*, 444 p.
- JACKSON, C.A.L., ZAKARIA, A.A., JOHNSON, H.D., TONGKUL, F., and CREVELLO, P.D., 2009, *Sedimentology, stratigraphic occurrence and origin of linked debrites in the West*

- Crocker Formation (Oligo-Miocene), Sabah, NW Borneo: *Marine and Petroleum Geology*, v. 26, p. 1957-1973.
- JAMES, D.M.D., 1984, *The Geology and Hydrocarbon Resources of Negara Brunei Darussalam*: Brunei Museum and Brunei Shell Petroleum Company, 169 p.
- JOHNSON, H.D., KUUD, T., and DUNDANG, A., 1989, Sedimentology and reservoir geology of the Betty field, Baram Delta Province, offshore Sarawak, NW Borneo: *Geological Society of Malaysia, Bulletin*, v. 25, p. 119-161.
- KVALE, E.P., ARCHER, A.W., and JOHNSON, H.R., 1989, Daily, monthly, and yearly tidal cycles within laminated siltstones of the Mansfield Formation (Pennsylvanian) of Indiana: *Geology*, v. 17, p. 365-368.
- KVALE, E.P., 2012, Tidal constituents of modern and ancient tidal rhythmites: criteria for recognition and analyses, *in* Davis, R.A., and Dalrymple, R.W., eds., *Principles of Tidal Sedimentology*: New York, Springer, p. 1-17.
- LAMB, M.P., and MOHRIG, D., 2009, Do hyperpycnal-flow deposits record river-flood dynamics?: *Geology*, v. 37, p. 1067-1070.
- LAMBIASE, J.J., BIN ABDUL RAHIM, A.A., and PENG, C.Y., 2002, Facies distribution and sedimentary processes on the modern Baram Delta: implications for the reservoir sandstones of NW Borneo: *Marine and Petroleum Geology*, v. 19, p. 69-78.
- LAMBIASE, J.J., DAMIT, A.R., SIMMONS, M.D., ABDOERRIAS, R., and HUSSIN, A., 2003, A depositional model and the stratigraphic development of modern and ancient tide-dominated deltas in NW Borneo, *in* Sidi, F.H., Nummedal, D., Imbert, P., Darman, H., and Posamentier, H.W., eds., *Tropical Deltas of Southeast Asia – Sedimentology, Stratigraphy, and Petroleum Geology*: SEPM, Special Publication 76, p. 109-123.
- LAMBIASE, J.J., and CULLEN, A.B., 2013, Sediment supply systems of the Champion “Delta” of NW Borneo: Implications for deepwater reservoir sandstones: *Journal of Asian Earth Sciences*, v. 76, p. 356-371.
- LEGLER, B., JOHNSON, H.D., HAMPSON, G.J., MASSART, B.Y.G., JACKSON, C.A.L., JACKSON, M.D., EL-BARKOOKY, A., and RAVNÅS, R., 2013, Facies model of a fine-grained, tide-dominated delta: Lower Dir Abu Lifa Member (Eocene), Western Desert, Egypt: *Sedimentology*, v. 60, p. 1313-1356.
- LEGLER, B., HAMPSON, G.J., JACKSON, C.A.L., JOHNSON, H.D., MASSART, B.Y.G., SARGINSON, M., and RAVNÅS, R., 2014, Facies relationships and stratigraphic architecture of distal, mixed tide- and wave-influenced deltaic deposits: Lower Segeo Sandstone, Western Colorado, U.S.A: *Journal of Sedimentary Research*, v. 84, p. 605-625.
- LEVELL, B.K., 1987, The nature and significance of regional unconformities in the hydrocarbon-bearing Neogene sequences offshore West Sabah: *Geological Society of Malaysia, Bulletin*, v. 21, p. 55-90.
- LI, W., BHATTACHARYA, J.P., and WANG, Y., 2011, Delta asymmetry: Concepts, characteristics, and depositional models: *Petroleum Science*, v. 8, p. 278-289.
- LI, Z., BHATTACHARYA, J.P., and SCHIEBER, J., 2015, Evaluating along-strike variation using thin-bedded facies analysis, Upper Cretaceous Ferron Notom Delta, Utah: *Sedimentology*, v. 62, p. 2060-2089.
- MACEachern, J.A., BANN, K.L., BHATTACHARYA, J.P., and HOWELL, C.D., 2005, Ichnology of deltas: organism responses to the dynamic interplay of rivers, waves, storms, and tides, *in* Giosan, L., and Bhattacharya, J.P., eds., *River Deltas—Concepts, Models, and Examples*: SEPM, Special Publication 83, p. 45-85.
- MACEachern, J.A., and BANN, K.L., 2008, The role of ichnology in refining shallow marine facies models, *in* Hampson, G.J., Steel, R.J., Burgess, P.M., and Dalrymple, R.W.,

- eds., *Recent Advances in Models of Siliciclastic Shallow-Marine Stratigraphy*: SEPM, Special Publication 90, p. 73-116.
- MACKAY, D.A., and DALRYMPLE, R.W., 2011, Dynamic mud deposition in a tidal environment: The record of Fluid-Mud deposition in the Cretaceous Bluesky Formation, Alberta, Canada: *Journal of Sedimentary Research*, v. 81, p. 901-920.
- MADON, M.B., 1994, The stratigraphy of northern Labuan, NW Sabah Basin, East Malaysia: *Geological Society Of Malaysia, Bulletin*, v. 36, p. 19-30.
- MATHEW, M.J., MENIER, D., SIDDIQUI, N., KUMAR, S.G., and AUTHEMAYOU, C., 2016a, Active tectonic deformation along rejuvenated faults in tropical Borneo: Inferences obtained from tectono-geomorphic evaluation: *Geomorphology*, v. 267, p. 1-15.
- MATHEW, M.J., MENIER, D., SIDDIQUI, N., RAMKUMAR, M., SANTOSH, M., KUMAR, S., and HASSAAN, M., 2016b, Drainage basin and topographic analysis of a tropical landscape: Insights into surface and tectonic processes in northern Borneo: *Journal of Asian Earth Sciences*, v. 124, p. 14-27.
- MENIER, D., MATHEW, M., PUBELLIER, M., SAPIN, F., DELCAILLAU, B., SIDDIQUI, N., RAMKUMAR, M., and SANTOSH, M., 2017, Landscape response to progressive tectonic and climatic forcing in NW Borneo: Implications for geological and geomorphic controls on flood hazard: *Scientific Reports*, v. 7, Article number 457.
- MIALL, A.D., 1991, Hierarchies of architectural units in terrigenous clastic rocks, and their relationship to sedimentation rate, *in* Miall, A.D., and Tyler, N., eds., *The Three-Dimensional Facies Architecture of Terrigenous Clastic Sediments and Its Implications for Hydrocarbon Discovery and Recovery*: SEPM, *Concepts in Sedimentology and Paleontology*, no. 3, p. 6-12.
- MIALL, A.D., 2015, Updating uniformitarianism: stratigraphy as just a set of 'frozen accidents', *in* Smith, D.G., Bailey, R.J., Burgess, P.M., and Fraser, A.J., eds., *Strata and Time: Probing the Gaps in Our Understanding*: Geological Society of London, Special Publication 404, p. 11-36.
- MILLER, K.G., KOMINZ, M.A., BROWNING, J.V., WRIGHT, J.D., MOUNTAIN, G.S., KATZ, M.E., SUGARMAN, P.J., CRAMER, B.S., CHRISTIE-BLICK, N., and PEKAR, S.F., 2005, The Phanerozoic record of global sea-level change: *Science*, v. 310, p. 1293-1298.
- MORLEY, C.K., BACK, S., VAN RENSBERGEN, P., CREVELLO, P., and LAMBIASE, J.J., 2003, Characteristics of repeated, detached, Miocene–Pliocene tectonic inversion events, in a large delta province on an active margin, Brunei Darussalam, Borneo: *Journal of Structural Geology*, v. 25, p. 1147-1169.
- MORLEY, C.K., and BACK, S., 2008, Estimating hinterland exhumation from late orogenic basin volume, NW Borneo: *Geological Society of London, Journal*, v. 165, p. 353-366.
- MOSS, S.J., 1998, Embaluh Group turbidites in Kalimantan: evolution of a remnant oceanic basin in Borneo during the Late Cretaceous to Palaeogene: *Geological Society of London, Journal*, v. 155, p. 509-524.
- MULHERN, J.S., JOHNSON, C.L., and MARTIN, J.M., 2017, Is barrier island morphology a function of tidal and wave regime?: *Marine Geology*, v. 387, p. 74-84.
- MURTAZA, M., RAHMAN, A.H.A., SUM, C.W., and KONJING, Z., 2018, Facies associations, depositional environments and stratigraphic framework of the Early Miocene–Pleistocene successions of the Mukah–Balingian Area, Sarawak, Malaysia: *Journal of Asian Earth Sciences*, v. 152, p. 23-38.
- NANSON, R.A., VAKARELOV, B.K., AINSWORTH, R.B., WILLIAMS, F.M., and PRICE, D.M., 2013, Evolution of a Holocene, mixed-process, forced regressive shoreline: the Mitchell River delta, Queensland, Australia: *Marine Geology*, v. 339, p. 22-43.

- NIENHUIS, J.H., ASHTON, A.D., ROOS, P.C., HULSCHER, S.J.M.H., and GIOSAN, L., 2013, Wave reworking of abandoned deltas: *Geophysical Research Letters*, v. 40, p. 5899-5903.
- NIO, S.-D., and YANG, C.-S., 1991, Diagnostic attributes of clastic tidal deposits: a review, *in* Smith, D., Reinson, G.G.E., Zaitlin, B.A., and Rahmani, R.A., eds., *Clastic Tidal Sedimentology*, Canadian Society of Petroleum Geologists, Memoir 16, p. 3-27.
- NYBERG, B., and HOWELL, J.A., 2015, Is the present the key to the past? A global characterization of modern sedimentary basins: *Geology*, v. 43, p. 643-646.
- NYBERG, B., and HOWELL, J.A., 2016, Global distribution of modern shallow marine shorelines. Implications for exploration and reservoir analogue studies: *Marine and Petroleum Geology*, v. 71, p. 83-104.
- OOMKENS, E., 1974, Lithofacies relations in the Late Quaternary Niger delta complex: *Sedimentology*, v. 21, p. 195-222.
- ORTON, G.J., and READING, H.G., 1993, Variability of deltaic processes in terms of sediment supply, with particular emphasis on grain size: *Sedimentology*, v. 40, p. 475-512.
- PENLAND, S., SUTER, J.R., and BOYD, R., 1985, Barrier island arcs along abandoned Mississippi River deltas: *Marine Geology*, v. 63, p. 197-233.
- PENLAND, S., BOYD, R., and SUTER, J.R., 1988, Transgressive depositional systems of the Mississippi delta plain: a model for barrier shoreline and shelf sand development: *Journal of Sedimentary Petrology*, v. 58, p. 932-949.
- PLINK-BJÖRKLUND, P., 2012, Effects of tides on deltaic deposition: Causes and responses: *Sedimentary Geology*, v. 279, p. 107-133.
- PLINT, A.G., 2014, Mud dispersal across a Cretaceous prodelta: Storm-generated, wave-enhanced sediment gravity flows inferred from mudstone microtexture and microfacies: *Sedimentology*, v. 61, p. 609-647.
- POMAR, L., MORSILLI, M., HALLOCK, P., and BÁDENAS, B., 2012, Internal waves, an under-explored source of turbulence events in the sedimentary record: *Earth-Science Reviews*, v. 111, p. 56-81.
- READING, H.G., and COLLINSON, J.D., 1996, *Clastic coasts*, *in* Reading, H.G., ed., *Sedimentary Environments; Processes, Facies and Stratigraphy*: Oxford, UK, Blackwell Science Ltd, p. 154-231.
- REINECK, H.-E., 1963, Sedimentgefüge im Bereich der südlichen Nordsee, *Senckenbergische Naturforschende Gesellschaft*, no. 505, *Abhandlungen*, 90 p.
- ROBERTS, H.H., and COLEMAN, J.M., 1996, Holocene evolution of the deltaic plain: a perspective—from Fisk to present: *Engineering Geology*, v. 45, p. 113-138.
- ROSSI, V.M., and STEEL, R.J., 2016, The role of tidal, wave and river currents in the evolution of mixed-energy deltas: Example from the Lajas Formation (Argentina): *Sedimentology*, v. 63, p. 824–864.
- SANDAL, S.T., 1996, The geology and hydrocarbon resources of Negara Brunei Darussalam: Bandar Seri Begawan, Brunei Darussalam, Brunei Shell Petroleum Company, Brunei Museum, 243 p.
- SCHIEBER, J., SOUTHARD, J.B., and THAISEN, K., 2007, Accretion of mudstone beds from migrating floccule ripples: *Science*, v. 318, p. 1760-1763.
- SHIERS, M.N., MOUNTNEY, N.P., HODGSON, D.M., and COBAIN, S.L., 2014, Depositional controls on tidally influenced fluvial successions, Neslen Formation, Utah, USA: *Sedimentary Geology*, v. 311, p. 1-16.
- SHORT, A.D., 2006, Australian beach systems—nature and distribution: *Journal of Coastal Research*, p. 11-27.
- SIMMONS, M.D., BIDGOOD, M.D., BRENAC, P., CREVELLO, P.D., LAMBIASE, J.J., and MORLEY, C.K., 1999, Microfossil assemblages as proxies for precise

- palaeoenvironmental determination—an example from Miocene sediments of northwest Borneo, *in* Jones, R.W., and Simmons, M.D., eds., *Biostratigraphy in Production and Development Geology*: Geological Society of London, Special Publication 152, p. 219-241.
- SIXSMITH, P.J., HAMPSON, G.J., GUPTA, S., JOHNSON, H.D., and FOFANA, J.F., 2008, Facies architecture of a net transgressive sandstone reservoir analog: The Cretaceous Hosta Tongue, New Mexico: *American Association of Petroleum Geologists, Bulletin*, v. 92, p. 513-547.
- SØMME, T.O., HOWELL, J.A., HAMPSON, G.J., and STORMS, J.E.A., 2008, Genesis, architecture, and numerical modeling of intra-parasequence discontinuity surfaces in wave-dominated deltaic deposits: Upper Cretaceous Sunnyside Member, Blackhawk Formation, Book Cliffs, Utah, USA, *in* Hampson, G.J., Steel, R.J., Burgess, P.M., and Dalrymple, R.W., eds., *Recent Advances in Models of Siliciclastic Shallow-Marine Stratigraphy*: SEPM, Special Publication 90, p. 421-441.
- SØMME, T.O., HELLAND-HANSEN, W., MARTINSEN, O.J., and THURMOND, J.B., 2009, Relationships between morphological and sedimentological parameters in source-to-sink systems: a basis for predicting semi-quantitative characteristics in subsurface systems: *Basin Research*, v. 21, p. 361-387.
- STORMS, J.E.A., 2003, Event-based stratigraphic simulation of wave-dominated shallow-marine environments: *Marine Geology*, v. 199, p. 83-100.
- STORMS, J.E.A., and HAMPSON, G.J., 2005, Mechanisms for forming discontinuity surfaces within shoreface–shelf parasequences: sea level, sediment supply, or wave regime?: *Journal of Sedimentary Research*, v. 75, p. 67-81.
- STOUTHAMER, E., and BERENDSEN, H.J.A., 2007, Avulsion: the relative roles of autogenic and allogenic processes: *Sedimentary Geology*, v. 198, p. 309-325.
- SWENSON, J.B., 2005, Relative importance of fluvial input and wave energy in controlling the timescale for distributary-channel avulsion: *Geophysical Research Letters*, v. 32, p. L23404.
- SWIFT, D.J.P., and THORNE, J.A., 1991, Sedimentation on continental margins I: A general model for shelf sedimentation, *in* Swift, D.J.P., Oertel, G.F., Tillman, R.W., and Thorne, J.A., eds., *Shelf Sand and Sandstone Bodies: Geometry, Facies and Sequence Stratigraphy*: International Association of Sedimentologists, Special Publication 14, p. 3-31.
- TA, T.K.O., NGUYEN, V.L., TATEISHI, M., KOBAYASHI, I., SAITO, Y., and NAKAMURA, T., 2002, Sediment facies and Late Holocene progradation of the Mekong River Delta in Bentre Province, southern Vietnam: an example of evolution from a tide-dominated to a tide- and wave-dominated delta: *Sedimentary Geology*, v. 152, p. 313-325.
- TA, T.K.O., NGUYEN, V.L., TATEISHI, M., KOBAYASHI, I., and SAITO, Y., 2005, Holocene delta evolution and depositional models of the Mekong River Delta, southern Vietnam, *in* Giosan, L., and Bhattacharya, J.P., eds., *River Deltas—Concepts, Models, and Examples*: SEPM, Special Publication 18, p. 453-466.
- TAMURA, T., and MASUDA, F., 2005, Bed thickness characteristics of inner-shelf storm deposits associated with a transgressive to regressive Holocene wave-dominated shelf, Sendai coastal plain, Japan: *Sedimentology*, v. 52, p. 1375-1395.
- TAMURA, T., SAITO, Y., NGUYEN, V.L., TA, T.O., BATEMAN, M.D., MATSUMOTO, D., and YAMASHITA, S., 2012, Origin and evolution of interdistributary delta plains: insights from Mekong River delta: *Geology*, v. 40, p. 303-306.
- TANABE, S., TA, T.K.O., NGUYEN, V.L., TATEISHI, M., KOBAYASHI, I., and SAITO, Y., 2003, Delta evolution model inferred from the Holocene Mekong Delta, southern Vietnam, *in* Sidi, F.H., Nummedal, D., Imbert, P., Darman, H., and Posamentier, H.W., eds.,

- Tropical Deltas of Southeast Asia—Sedimentology, Stratigraphy, and Petroleum Geology: SEPM, Special Publication 76, p. 175–188.
- TAYLOR, A., and GOLDRING, R., 1993, Description and analysis of bioturbation and ichnofabric: *Geological Society of London, Journal*, v. 150, p. 141-148.
- TAYLOR, A., GOLDRING, R., and GOWLAND, S., 2003, Analysis and application of ichnofabrics: *Earth-Science Reviews*, v. 60, p. 227-259.
- THOM, B.G., and WRIGHT, L.D., 1983, Geomorphology of the Purari Delta, *in* Petr, T., ed., *The Purari—Tropical Environment of a High Rainfall River Basin*: Dordrecht, Springer Netherlands, p. 47-65.
- THORNE, J.A., GRACE, E., SWIFT, D.J.P., and NIEDORODA, A., 1991, Sedimentation on Continental Margins, III: The depositional fabric—an analytical approach to stratification and facies identification, *in* Swift, D.J.P., Oertel, G.F., Tillman, R.W., and Thorne, J.A., eds., *Shelf Sand and Sandstone Bodies: Geometry, Facies and Sequence Stratigraphy*: International Association of Sedimentologists, Special Publication 14, p. 59-87.
- VAKARELOV, B.K., and AINSWORTH, R.B., 2011, Predicting marginal marine reservoir architecture: Examples from Asian shoreline systems: *International Petroleum Technology Conference (IPTC) 14472*.
- VAKARELOV, B.K., AINSWORTH, R.B., and MACEACHERN, J.A., 2012, Recognition of wave-dominated, tide-influenced shoreline systems in the rock record: Variations from a microtidal shoreline model: *Sedimentary Geology*, v. 279, p. 23-41.
- VAKARELOV, B.K., and AINSWORTH, R.B., 2013, A hierarchical approach to architectural classification in marginal-marine systems: Bridging the gap between sedimentology and sequence stratigraphy: *American Association of Petroleum Geologists, Bulletin*, v. 97, p. 1121-1161.
- VAN CAPPELLE, M., STUKINS, S., HAMPSON, G.J., and JOHNSON, H.D., 2016, Fluvial to tidal transition in proximal, mixed tide-influenced and wave-influenced deltaic deposits: Cretaceous lower Sego Sandstone, Utah, USA: *Sedimentology*, v. 63, p. 1333–1361.
- VAN CAPPELLE, M., RAVNÅS, R., HAMPSON, G.J., and JOHNSON, H.D., 2017, Depositional evolution of a progradational to aggradational, mixed-influenced deltaic succession: Jurassic Tofte and Ile formations, southern Halten Terrace, offshore Norway: *Marine and Petroleum Geology*, v. 80, p. 1-22.
- VAN HATTUM, M.W.A., HALL, R., PICKARD, A.L., and NICHOLS, G.J., 2013, Provenance and geochronology of Cenozoic sandstones of northern Borneo: *Journal of Asian Earth Sciences*, v. 76, p. 266-282.
- VAN WAGONER, J.C., MITCHUM, R.M., CAMPION, K.M., and RAHMANIAN, V.D., 1990, Siliciclastic Sequence Stratigraphy in Well Logs, Cores, and Outcrops: Concepts for High-Resolution Correlation of Time and Facies: *American Association of Petroleum Geologists, Methods in Exploration*, v. 7, 55 p.
- VAN WAGONER, J.C., 1991, High-frequency sequence stratigraphy and facies architecture of the Sego Sandstone in the Book Cliffs of western Colorado and eastern Utah, *in* Van Wagoner, J.C., Nummedal, D., Jones, C.R., Taylor, D.R., Jennette, D.C., and Riley, G.W., eds., *Sequence Stratigraphy—Applications to Shelf Sandstone Reservoirs Outcrop to Subsurface Examples*: American Association of Petroleum Geologists Field Conference Guidebook, p. 1–22.
- VERSTAPPEN, H.T., 1975, On palaeo-climate and landform development in Malesia: *Modern Quaternary Research in Southeast Asia*, v. 1, p. 3-36.
- WARNE, A.G., MEADE, R.H., WHITE, W.A., GUEVARA, E.H., GIBEAUT, J., SMYTH, R.C., ASLAN, A., and TREMBLAY, T., 2002, Regional controls on geomorphology,

- hydrology, and ecosystem integrity in the Orinoco Delta, Venezuela: *Geomorphology*, v. 44, p. 273-307.
- WHEATCROFT, R.A., 2000, Oceanic flood sedimentation: a new perspective: *Continental Shelf Research*, v. 20, p. 2059-2066.
- WHEATCROFT, R.A., and DRAKE, D.E., 2003, Post-depositional alteration and preservation of sedimentary event layers on continental margins, I. The role of episodic sedimentation: *Marine Geology*, v. 199, p. 123-137.
- WILLIS, B.J., BHATTACHARYA, J.P., GABEL, S.L., and WHITE, C.D., 1999, Architecture of a tide-influenced river delta in the Frontier Formation of central Wyoming, USA: *Sedimentology*, v. 46, p. 667-688.
- WOLANSKI, E.E.J., MAZDA, Y.Y., and RIDD, P.P.V., 1992, Mangrove hydrodynamics, *in* Robertson, A.I., and Alongi, D.M., eds., *Tropical Mangrove Ecosystems: American Geophysical Union, Coastal and Estuarine Studies*, v. 41, p. 43-62.
- WOODROFFE, C.D., ROGERS, K., MCKEE, K.L., LOVELOCK, C.E., MENDELSSOHN, I.A., and SAINTILAN, N., 2016, Mangrove sedimentation and response to relative sea-level rise: *Annual Review of Marine Science*, v. 8, p. 243-66.
- YOSHIDA, S., JOHNSON, H.D., PYE, K., and DIXON, R.J., 2004, Transgressive changes from tidal estuarine to marine embayment depositional systems: The Lower Cretaceous Woburn Sands of southern England and comparison with Holocene analogs: *American Association of Petroleum Geologists Bulletin*, v. 88, p. 1433-1460.
- YOSHIDA, S., STEEL, R.J., and DALRYMPLE, R.W., 2007, Changes in depositional processes—an ingredient in a new generation of sequence-stratigraphic models: *Journal of Sedimentary Research*, v. 77, p. 447-460.
- ZAITLIN, B.A., DALRYMPLE, R.W., and BOYD, R., 1994, The stratigraphic organization of incised-valley systems associated with relative sea-level change, *in* Dalrymple, R.W., Zaitlin, B.A., and Boyd, R., eds., *Incised-Valley Systems: Origin and Sedimentary Sequences: SEPM, Special Publication 51*, p. 45-60.

FIGURE CAPTIONS

FIG. 1.—**A**) Location of the Baram Delta Province (BDP) in southeast Asia. **B**) Simplified hydrologic, topographic, and bathymetric map of the present-day BDP including the interpreted Middle Miocene to Pliocene shelf-edge positions (colored lines) derived from seismic data (Cullen 2010b; Lambiase and Cullen 2013). See Fig 11A for satellite image. **C**) Simplified geological map of the Berakas Syncline, eastern BDP (Brunei) (after Morley et al. 2003; Back et al. 2005) showing the positions of studied outcrops (red dots, 1–9). JF = Jerudong Fault; MF = Muara Fault. Informal outcrop location names: 1 = Sungai Kabun; 2 = Jalan Subok 422; 3 = Jalan Subok 247; 4 = Jalan Kampung Kianggeh; 5 = Jalan Tutong 688; 6 = Jalan Talani; 7 = Jalan Bunut; and 8 = Tanjong Nangka (see Supplementary Fig. 1).

FIG. 2.—**A**) Simplified stratigraphic log through FS 1 at location 5 (circled red numeral; Fig. 1C). Key is shown in Fig. 8. **B**) Heterolithic FS 1 with abundant gutter casts. Black line is log shown in part A. **C**) Isolated, rectangular steep-sided gutter cast. **D**) Multi-bed gutter-cast complex. **E**) FS 2 sandy heterolithics (F5a) with combined-flow-ripple cross-laminated sandstone, millimeter-scale mud flasers and drapes, and rare current-ripple cross-lamination (purple arrows). Location 7, c. 12 m (Supplementary Fig. 1H). **F**) Intense, moderate-diversity bioturbation (BI 4) in FS 2 muddy heterolithics (F4a). Location 3b, c. 9 m (Fig. 8C). **G**) Interstratified heterolithics (F4a and F5a) and very fine-grained sandstone (F6), which show concave-upwards erosional discontinuities (black arrows) and rare current ripples (purple arrows). Location 1, c. 20 m (Fig. 8B). **H**) Mud-draped SCS (blue arrows) and aggrading, asymmetric-combined-flow-ripple cross-lamination (red arrows) and lenses of trough-cross-stratified, fine-grained sandstone (F9a). Ichnogenera include *Asterosoma* (*As*), *Chondrites* (*Ch*), *Diplocraterion* (*Di*), *Ophiomorpha* (*Op*), *Palaeophycus tubularis* (*Pt*), *Planolites* (*P*), *Rosselia* (*R*), *Skolithos* (*S*), and *Thalassinoides* (*Th*).

FIG. 3.—**A**) Simplified stratigraphic log through FS 2 at location 7 (Fig. 1C). **B**) Line drawing of swaly cross-stratified sandstone (F6) in FS 2 (cf. Fig. 3A) showing (1) a hierarchy of discontinuity surfaces, (2) common asymmetry (black arrows), (3) interstratified coarser (fine-grained) sandstone (F9a), (4) subordinate intrastratified muddy heterolithics (F4a), and (5) extremely high preservation of physical stratification at all scales (sub-mm-scale upwards), with generally low (BI 0–1) but sporadically high (BI 3) bioturbation.

FIG. 4.—**A**) Upward-sanding FS 3 unit at location 8 (Fig. 1C). **B**) Muddy heterolithics (F4a) displaying sandstone layers with combined-flow ripple cross-lamination (red arrows) and bioturbation including *Asterosoma* (As), *Cylindrichnus* (Cy) and *Palaeophycus tubularis* (Pt), and top-down *Schaubcylindrichnus* modified by *Planolites* and *Skolithos* (white arrows). Location 7, c. 17 m (Fig. 8D). **C**) Sandy heterolithics (F5b) show mainly bidirectional-current-ripple cross-lamination and minor bioturbation. Combined-flow-ripple cross-lamination (red arrows) suggest increased wave reworking upwards. Location 7, c. 28 m (Fig. 8D). **D**) Photograph of inset area in Part A. **E**) Line drawing of photograph in Part D shaded for facies. Trough-cross-bedded sandstone (F9b), swaly cross-stratified sandstone (F6) and massive mudstone (F2a) sharply overlies and show gradual lateral transitions into sandy heterolithics (F5b).

FIG. 5.—**A**) FS 6 units with basal erosional surfaces (ES), which display lateral-accretion surfaces dipping in various directions, are sharply overlain by carbonaceous mudstone (FS 9). Location 3c, c. 6–12 m (Supplementary Fig. 1D) (cf. Figs. 8C, 10A–C). **B**) Sharp-based FS 6 units mainly comprising low-angle-laminated to planar-laminated sandstone with abundant

carbonaceous-rich laminae (F8d). Location 2, c. 31–33 m (Supplementary Fig. 1B). **C**) Trough-cross-bedded sandstone (F9a) in FS 6. Location 3b, c. 31.5 m (Fig. 8C). **D**) Carbonaceous laminae, coal layers and resting traces (white arrows) in F8d and F11b (refer to Fig. 5B). **E**) Climbing ($< 10^\circ$), carbonaceous-draped, current ripples (pink arrows) (F10b) in FS 6. Location 2, c. 32 m (Supplementary Fig. 1B). **F**) Sharp-based FS 7 units containing trough-cross-bedded sandstone (F9b) with abundant mud drapes and clasts and common carbonaceous clasts (green arrows). Location 7, c. 11 m (Fig. 8D). **G**) FS 7 unit sharply overlying FS 9 containing a coal horizon (hammer). **H**) Muddy heterolithics (F4b) with *Thalassinoides*-dominated bioturbation, including occasional centimeter- to decimeter-scale dwelling burrows (white arrow). Location 4, c. 12 m (Supplementary Fig. 1E). **I**) Coalified subhorizontal root in carbonaceous mudstone (F2b). YD = younging direction. Location 2, c. 17 m (Supplementary Fig. 1B). **J**) Massive muddy and carbonaceous sandstone sub-unit in F2b. Location 3a, c. 1 m (Fig. 8C).

FIG. 6.—**A**) Process interpretation of facies successions (FS) 1–9 (refer to Table 2 for FS classification) using a ternary plot for shoreline–shelf process classification (Ainsworth et al. 2011). Inset shows end-member and mixed-process color scheme used in this study. W = wave-dominated; F = river-dominated; T = tide-dominated; Upper case = dominant process, lower case = secondary process, lower-case italics = tertiary process, e.g., Fwt = river-dominated, wave-influenced, tide-affected. **B**) Process interpretations of facies succession sets (FSS) 1–3 and studied exposures (Fig. 1C and Supplementary Fig. 1).

FIG. 7.—Summary logs of facies succession sets (FSS) 1–3 interpreted in the Belait Formation, eastern Baram Delta Province. **A**) FSS 1: wave-dominated (storm-wave-

reworked) delta and flanking strandplain. **B**) FSS 2: mixed-process (storm-wave-reworked, river- and tide-influenced) delta and flanking strandplain. **C**) FSS 3: tide-dominated, wave- (storm-wave-reworked) and river-influenced, coastal embayment. Refer to Fig. 8 for log key.

FIG. 8.—Stratigraphic logs illustrating examples of the vertical distribution of facies (F), sand vs. shale (S-Sh), facies successions (FS 1–FS 9) and facies successions sets (FSS 1–FSS 3): **A**) c. 15 m of interpreted FSS 1 exposed at location 8 (Tanjong Nangka) (cf. Collins et al. 2017); **B**) c. 32 m of interpreted FSS 2 exposed at location 1; **C**) 40 m of exposed section at location 3; and **D**) c. 36 m of exposed section at location 7. Exposure locations are shown in Fig. 1C. Full stratigraphic logs are shown in Supplementary Fig. 1. Grain-size abbreviations: cl = clay; si = silt; vf = very fine; f = fine; m = medium. Refer to Table 1 for ichnogenera abbreviations.

FIG. 9.— Stratigraphic architecture in FSS 1 and FSS 2. **A**) Photograph of exposed section between c. 3 and 12 m of the stratigraphic log in Fig. 8A. **B**) Line drawing of photograph in Part A shaded for facies succession architecture (refer to Table 2 for classification of facies successions). **C**) Photograph of exposed section between c. 10 and 36 m of the stratigraphic log in Fig. 8B. Refer to Table 1 for ichnogenera abbreviations.

FIG. 10.—Stratigraphic architecture in FSS 2 and FSS 3. **A**) Photograph of the exposed section at location 3 (cf. Supplementary Fig. 1C, D). The sharp, horizontal lines (with apparent offset) are cut terraces without any geological offset which were created by civil-engineering excavation work. **B**) Interpreted facies-succession architecture for photograph in

Part A. The thick black line shows the position of the stratigraphic log shown in Fig. 8C. **C)** Photograph of exposed section between c. 11 and 40 m of the stratigraphic log in Fig. 8C and an area of Part A. Note the erosional gutter cast (red arrow) associated with FS 2 and the lateral-accretion surfaces (black arrows) associated with FS 6. **D)** Photograph of exposed section between c. 12 and 15 m of the stratigraphic log in Fig. 8D. **E)** Quartzite cobbles along the sharp base of FS 7 at 13.5 m (cf. Figs. 8C, 10D). **H)** Photograph of exposed section between c. 18 and 36 m of the stratigraphic log in Fig. 8D.

FIG. 11.—Present-day coastal–deltaic depositional system in the Baram Delta Province (BDP), showing the Baram River shelf delta and, along-strike, the flanking open-coastline strandplain and the Brunei Bay coastal embayment. **A)** Geomorphological features and interpreted depositional process environments. **B)** Interpretation of the equivalent facies successions (FS) preserved in the Middle–Late Miocene Belait Formation. Refer to Fig. 6A and Table 2 for process classification of facies successions.

FIG. 12.— **A)** Aerial photograph of the Niah River mouth, western Baram Delta Province (BDP), in 2007. The location is shown in Fig. 11A. **B)** Interpreted sediment distribution and morphology of the Niah River mouth in 2007. **C)** Google Earth satellite image of the Niah River mouth in 2013. **D)** Interpreted sediment distribution and morphology of the Niah River mouth in 2013. This type of “storm-flood”-related river-mouth switching is common throughout the Modern BDP (see also Collins et al. 2017).

FIG. 13.—Present-day coastal-embayment depositional system in Brunei Bay, eastern Baram Delta Province. **A)** Geomorphological features and location of sub-depositional systems (satellite image from Bing), including 1) Padas delta, 2) Mengalong delta, 3) Lawas delta, 4) Trusan delta, 5) Limbang delta, and 6) Muara spit. The dashed white line is the axis of a surface anticline along the Klias Peninsula that plunges southwestwards into the subsurface and across the subaqueous entrance of Brunei Bay (Abdul Razak 2001; Lambiase and Cullen 2013). **B)** Simplified and partly schematic map of interpreted process depositional environments and geomorphological elements. Key for geomorphological elements is shown below. Refer to Fig. 6A for ternary process diagram. **C)** Interpretation of equivalent facies successions (FS) preserved in the Middle–Late Miocene Belait Formation. Refer to Table 2 for classification of facies successions. After Abdul Razak (2001).

FIG. 14.—Map of Inner Brunei Bay showing depositional environments, bathymetry, and vibracore locations. Vibracore locations and numbers shown in red are included in this study (Fig. 15). See Fig. 13A for satellite image. After Abdul Razak (2001).

FIG. 15.—Photographs and summary sedimentological logs of vibracores from Inner Brunei Bay. Core number is shown in red, and core locations are shown in Fig. 14. **A)** Fluvio-tidal channel deposit, Limbang delta (core 56). **B)** Fluvio-tidal mouth-bar deposit, Limbang delta (core 20). **C)** Subtidal mudflat deposit, Limbang delta (core 23). **D)** Abandoned-tidal-channel deposit (core 107). **E)** Distributary-fluvio-tidal-channel deposit, Trusan delta (core 78). **F)** Active-channel-lobe deposit, Trusan delta (core 91). **G)** Mouth-bar deposit, Trusan delta (core 122). Photograph with blue border is of a core peel. **H)** Delta-front deposit, Trusan delta

(core 113). **I**) Interdistributary-bay deposit, Trusan delta (core 93). Ichnogenera include *Ophiomorpha* (*Op*), *Palaeophycus tubularis* (*Pt*), and *Teichichnus* (*T*).

FIG. 16.—Maps of sediment grain-size distribution maps of the offshore open coastline and Inner Brunei Bay, Baram Delta Province. **A**) Median grain diameter. **B**) Coarsest grain diameter. After Sandal (1996).

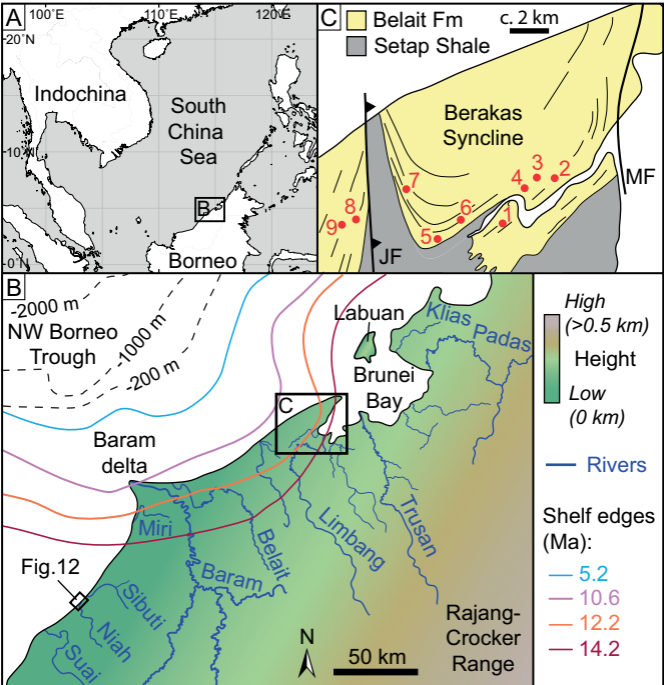
FIG. 17.— Depositional models for the Middle Miocene Belait Formation, eastern Baram Delta Province. **A**) Wave-dominated (storm-reworked), river-influenced and tide-affected (“storm-flood”-dominated), multi-sourced, open coastline (FSS 1) at time 1 (T1). **B**) Drainage-basin switching results in abrupt, along-strike changes in the volume of sediment supplied, including the formation of coeval, local, wave- and tide-influenced, transgressive barrier system (in areas of reduced sediment supply) and a new regressive deltaic depositional system at time 2 (T2). **C**) River- and wave-dominated, tide-affected open coastline (FSS 2) and relatively-low wave-energy, tide-influenced, slightly embayed coastal regions (FSS 3). **D**) Drainage-basin switching results in spatial changes in the distribution of FSS 2 and FSS 3 depositional systems. **E**) Regional transgression across the entire depositional system forms small drowned river mouths (converted to estuaries), larger drowned incised valleys and bays, and barrier-lagoon systems (FSS 3) with flanking wave-dominated strandplains (FSS 1–FSS 2). **F**) Structurally controlled embayments may form simultaneous wave-dominated (FSS 1–FSS 2) and tide-dominated (FSS 3) depositional systems (cf. Modern Brunei Bay). Forward slashes between facies succession sets and process classifications mean “and/or”.

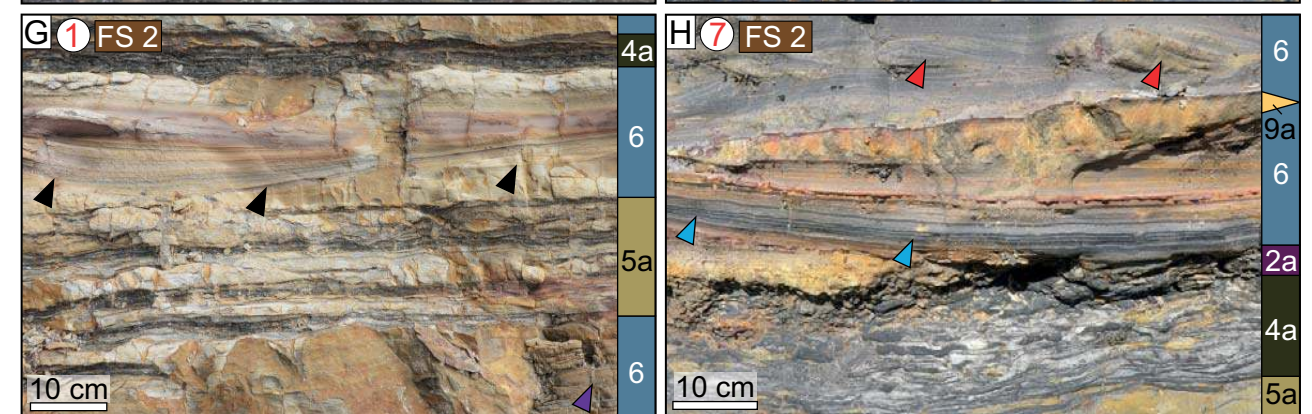
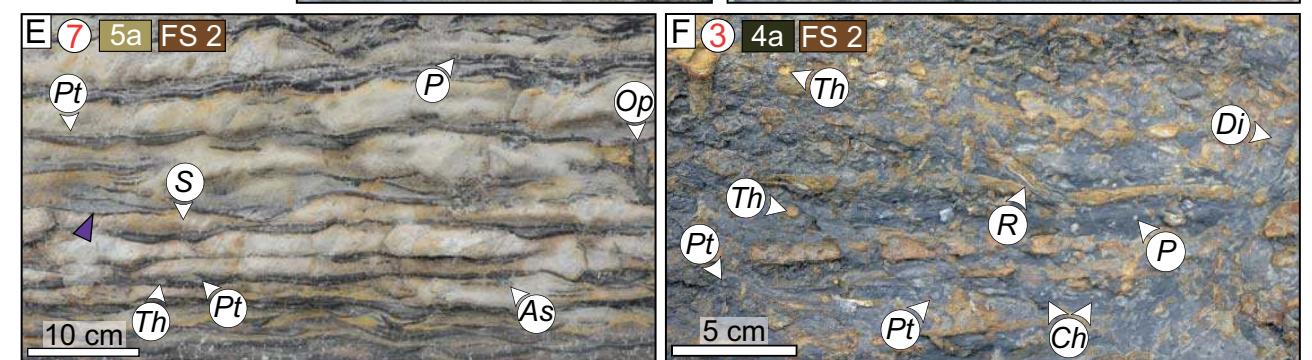
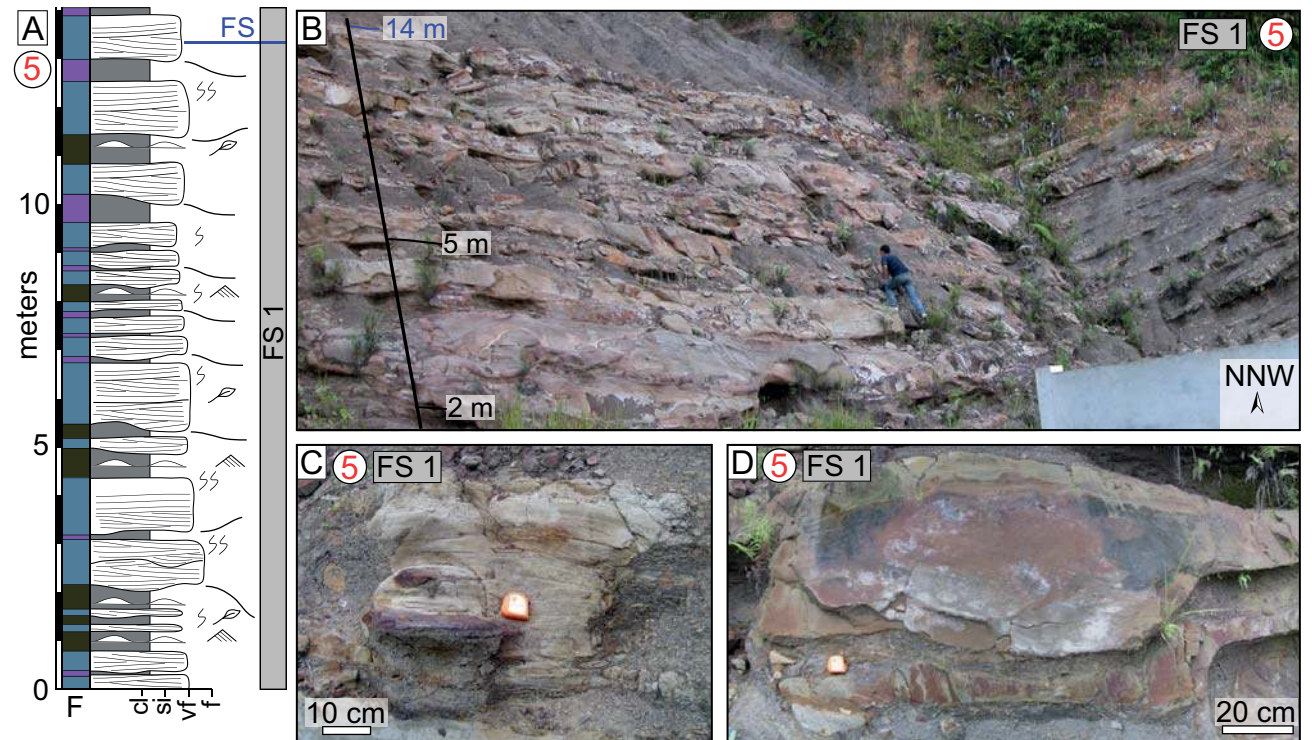
FIG. 18.— Processes controlling preservation of shoreline–shelf depositional systems. **A)** Rates and durations of processes controlling sediment deposition and erosion (after Miall 2015). Processes 1–6 are impacted by the relative strength of wave (W), fluvial (F), and tidal (T) processes. Refer to Miall (2015) for breakdown of processes 10–12. **B)** Schematic shoreline–shelf profile showing the approximate longitudinal zones of influence (pink lines) for processes 1–12 and, for processes 1–6, wave, fluvial, and tidal processes (thin black lines). Arrowed lines indicate extent of zone of influence. Dashed lines indicate uncertainty in extent of zone of influence. Open-ended lines indicates extension of the zone of influence outside the depicted area. Eustatic variations in mean sea level (MSL; blue arrow) are caused principally by processes 8 and 9 (e.g., Miller et al. 2005). FWWB = fairweather wave base. SWB = storm wave base. U = uplift. S = subsidence. **C)** Schematic plan view of a deltaic shoreline–shelf system showing the approximate areal zones of influence of processes 1–12. Tidal influence (processes 3–4) dominate in the seaward part of the fluvial-to-marine transition zone (FMTZ). Autogenic processes (7) are limited to single drainage basins whereas allogenic processes (8–12) can cause drainage-basin switching.

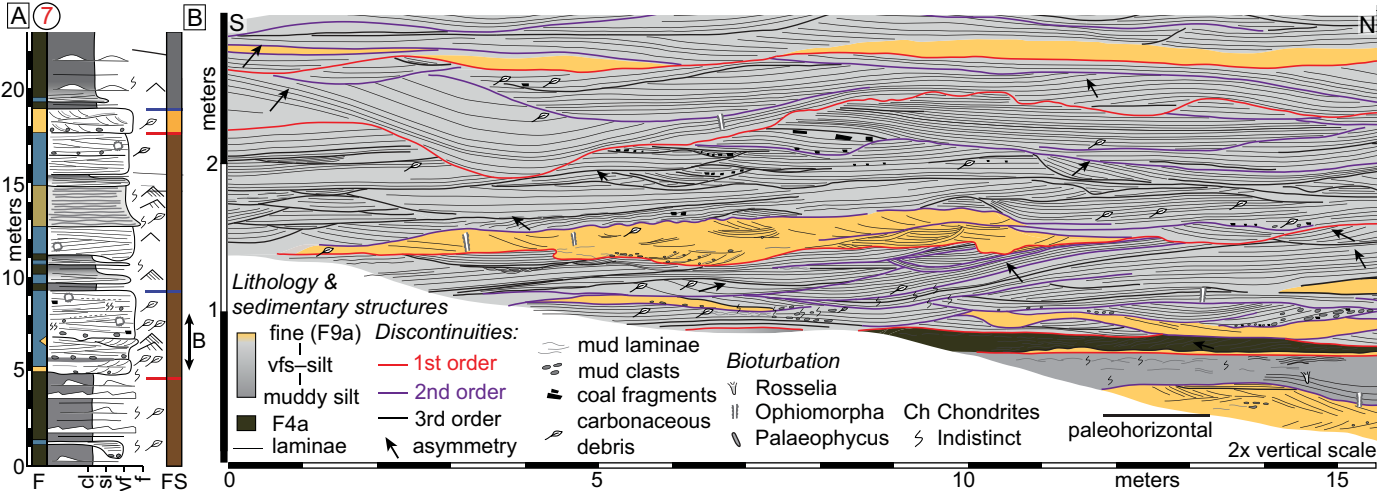
TABLE CAPTIONS

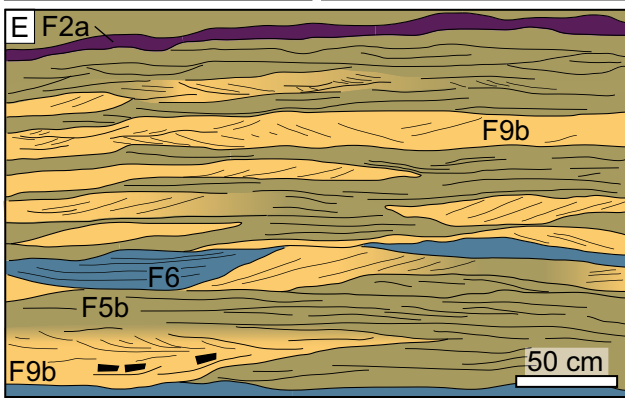
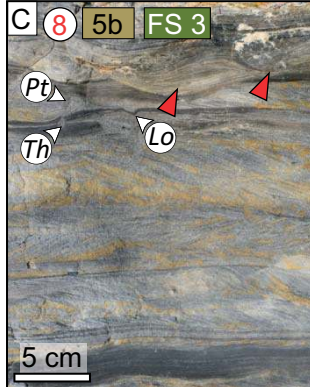
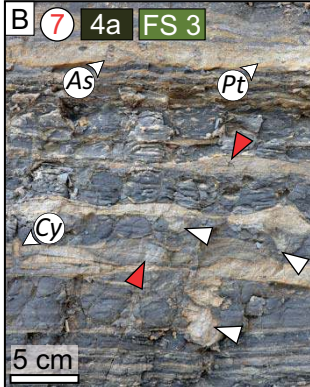
TABLE 1.—*Shoreline–shelf facies in the Belait Formation. Ichnogenera recognized include Asterosoma (As), Chondrites (Ch), Cylindrichnus (Cy), Diplocraterion (Di), Gyrolithes (Gy), Lockeia (Lo), Macaronichnus (Ma), Ophiomorpha (Op), Palaeophycus herbeti (Pa), Palaeophycus tubularis (Pt), Phycosiphon (Ph), Planolites (P), Rhizocorallium (Rz), Rosselia (R), Schaubcylindrichnus (Sh), Skolithos (S), Teichichnus (T), “Terebellina” (sensu lato) (Te), Thalassinoides (Th), collapse burrows (cb), and fugichnia (fu) (e.g., MacEachern and Bann 2008). Grain-size abbreviations: mst = mudstone; slst = siltstone; sst = sandstone; vf = very fine-grained; vfL = lower very fine-grained; vfU = upper very fine-grained; f = fine-grained. BI = bioturbation index.*

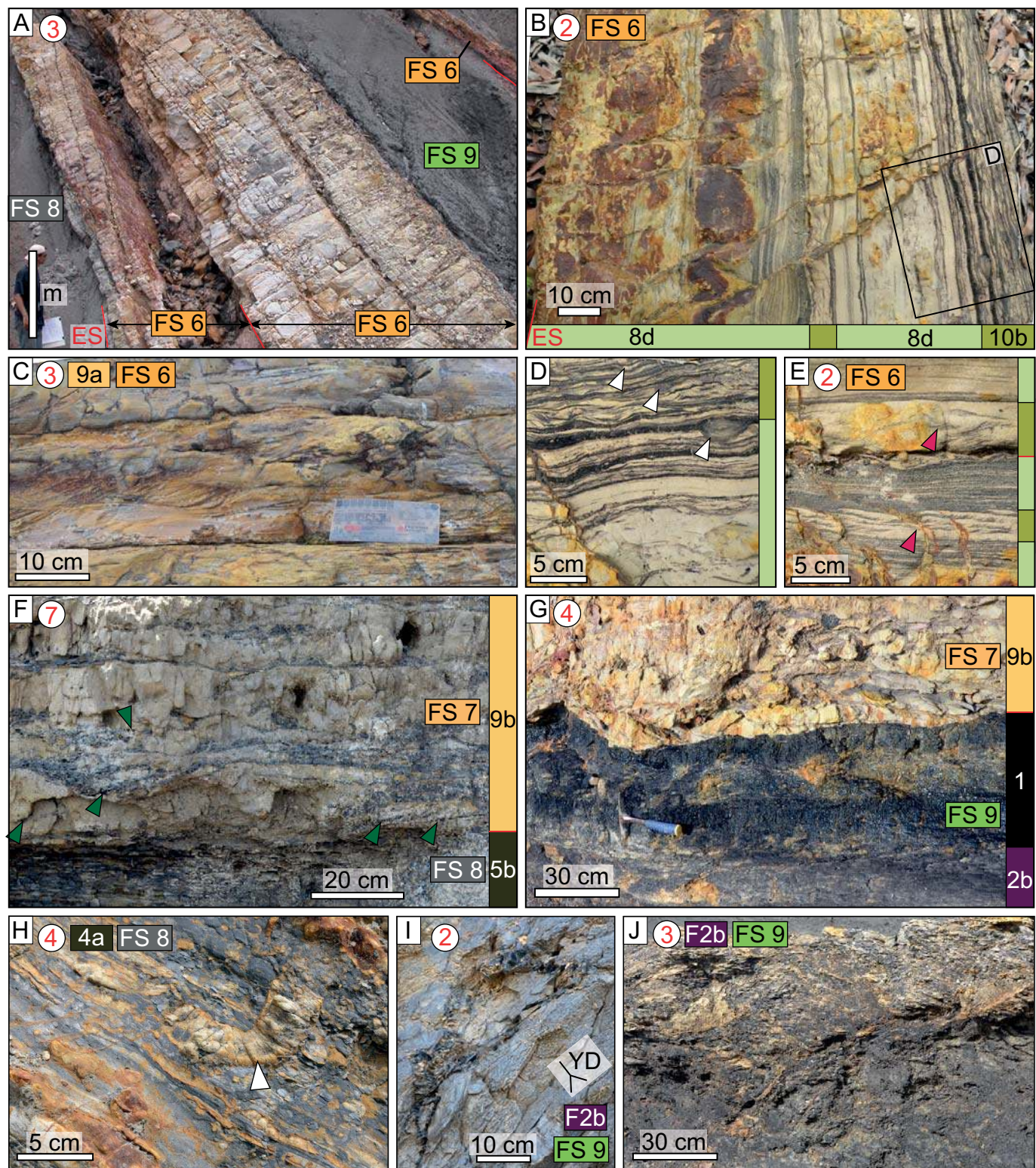
TABLE 2.—*Shoreline–shelf facies successions in the Belait Formation. Refer to Table 1 for facies classification and key.*



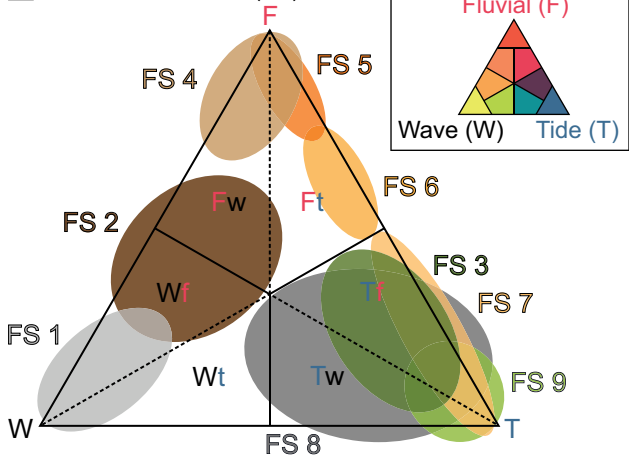




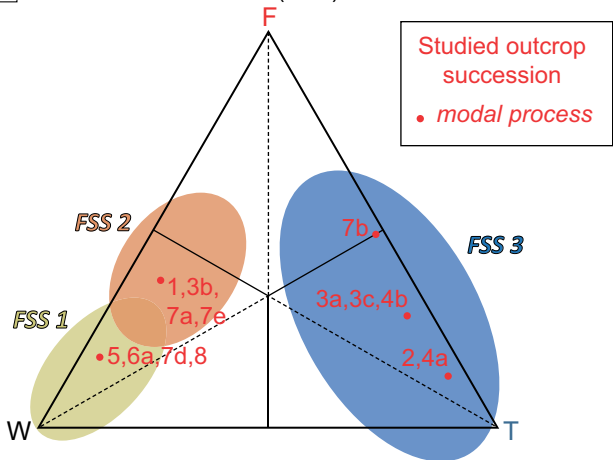




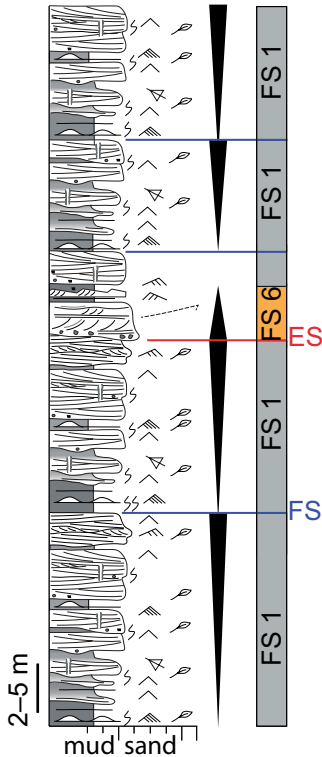
A Facies successions (FS)



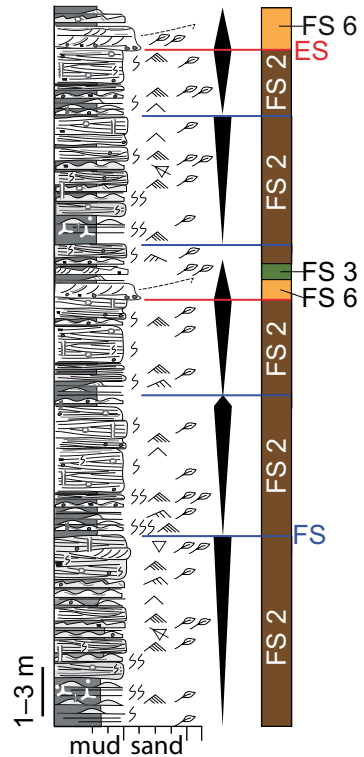
B Facies succession sets (FSS)



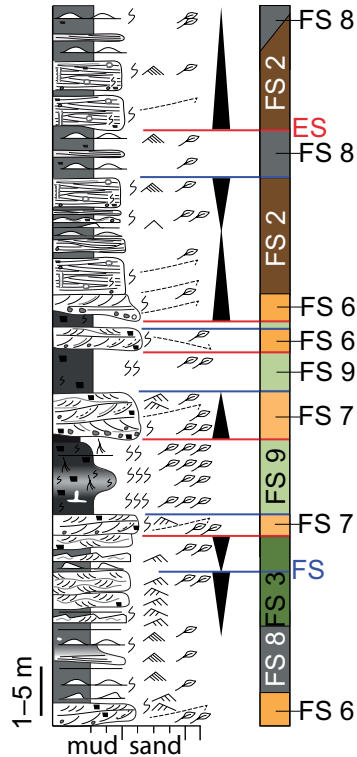
A **FSS 1** Wave-dominated delta and/or flanking strandplain

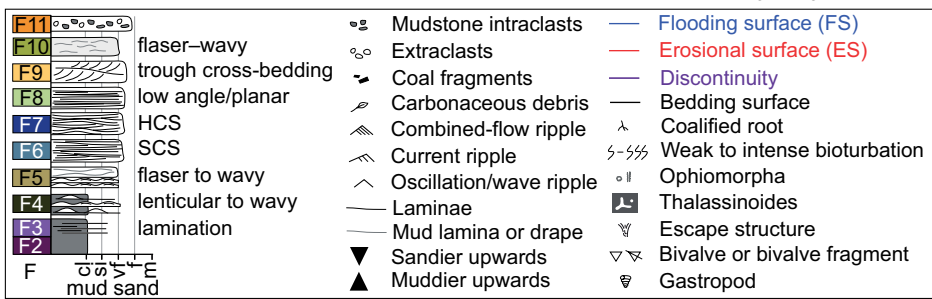
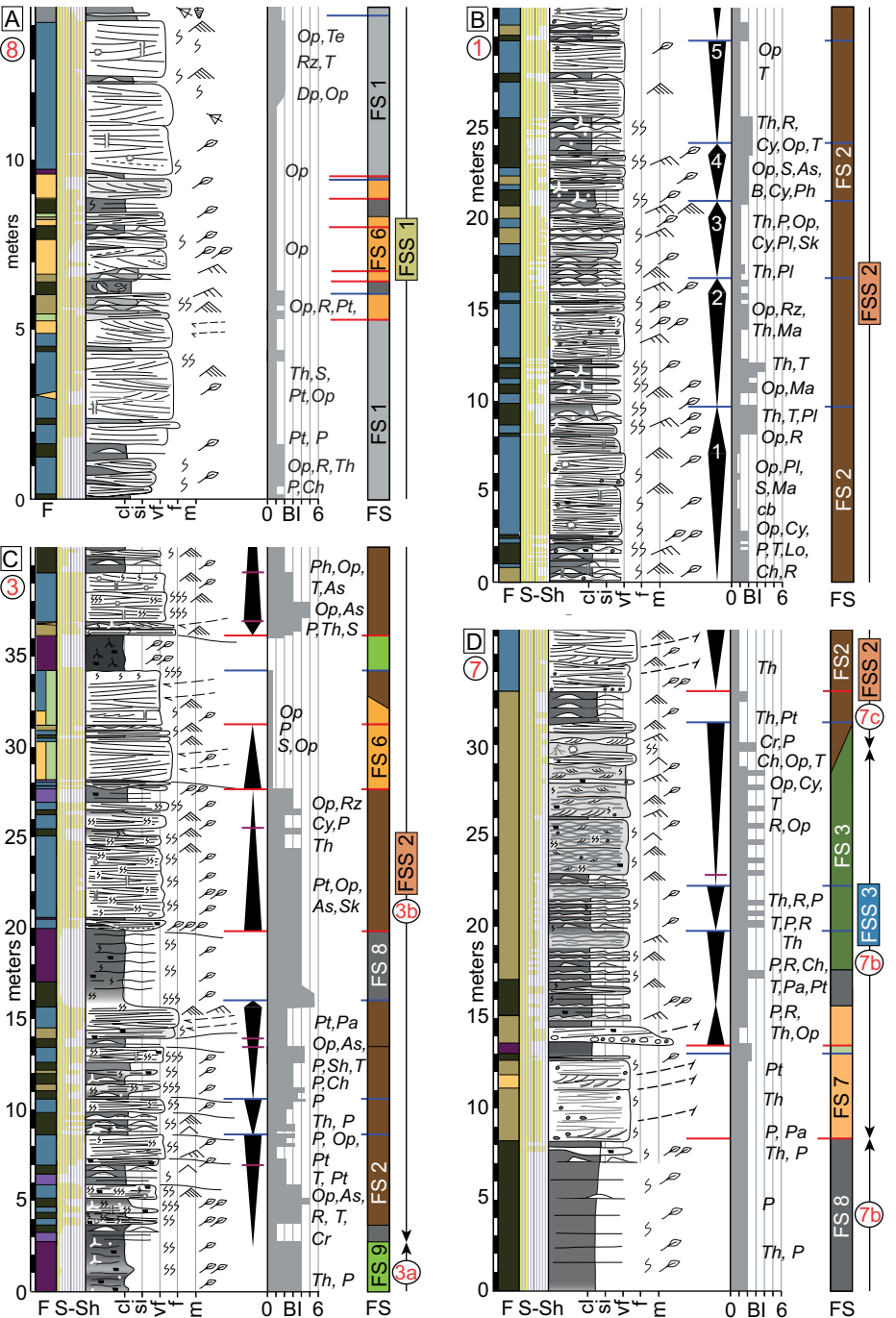


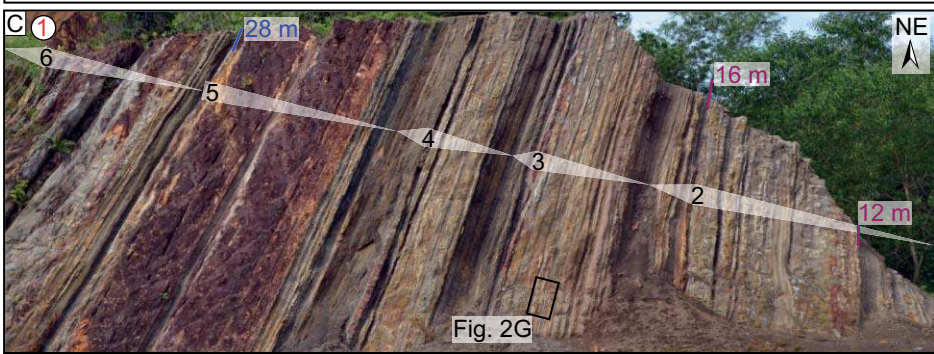
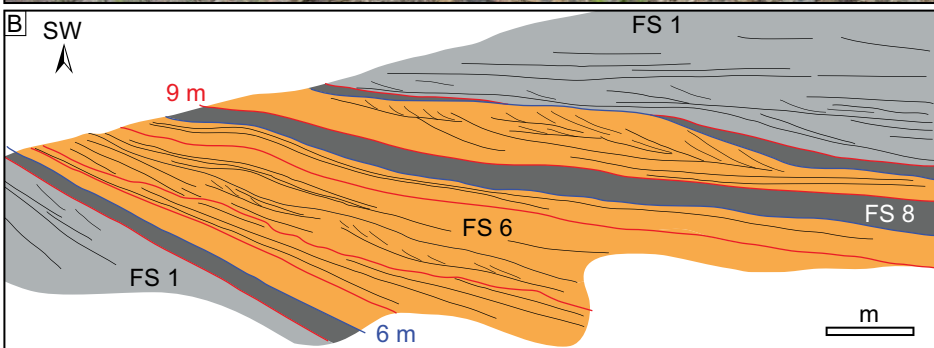
B **FSS 2** Mixed-process delta and/or flanking strandplain

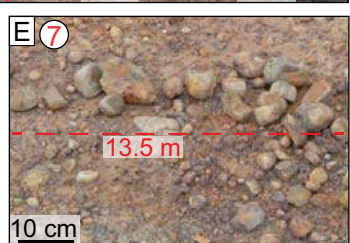
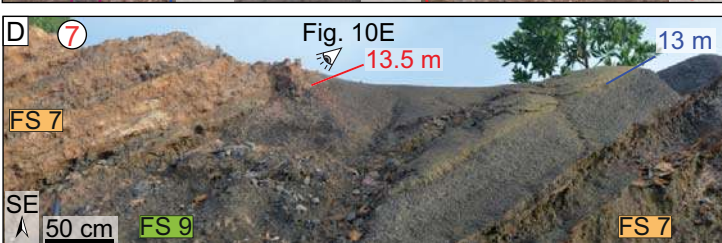
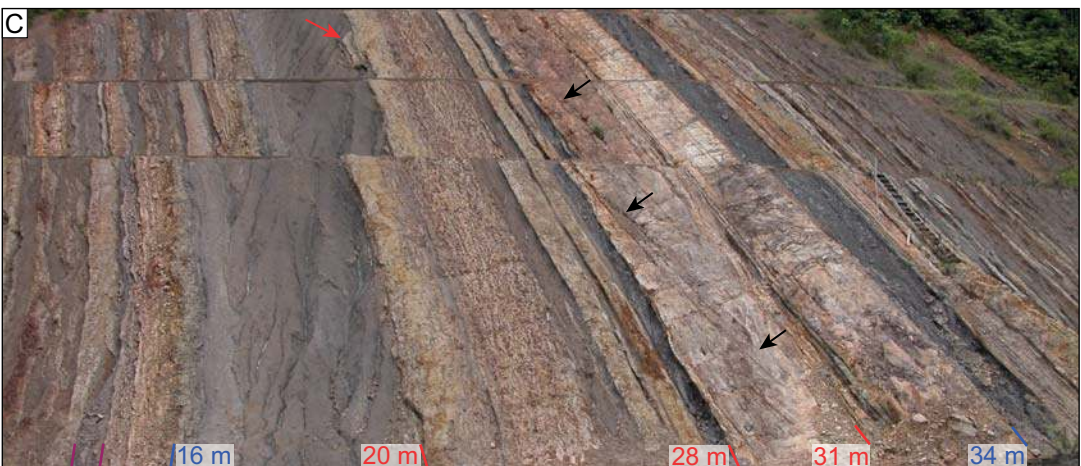
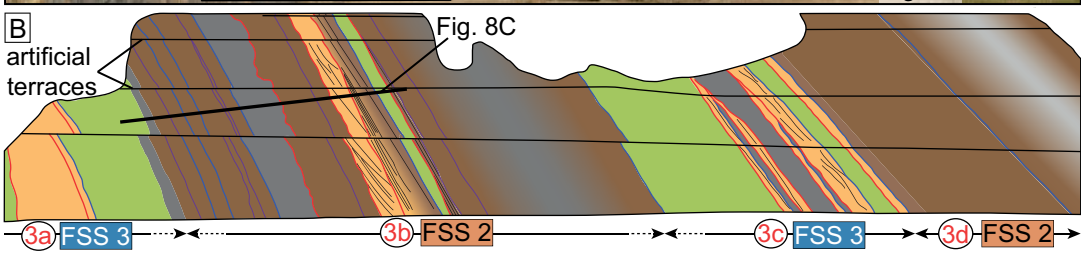
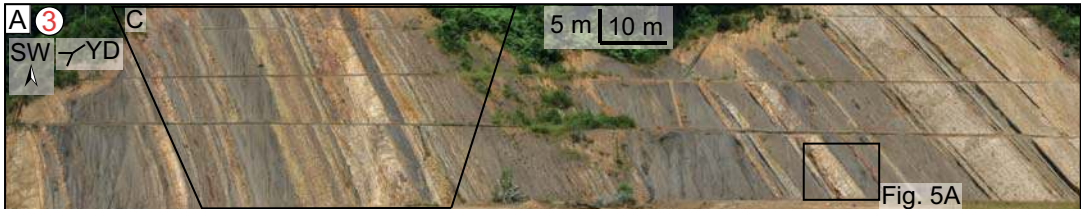


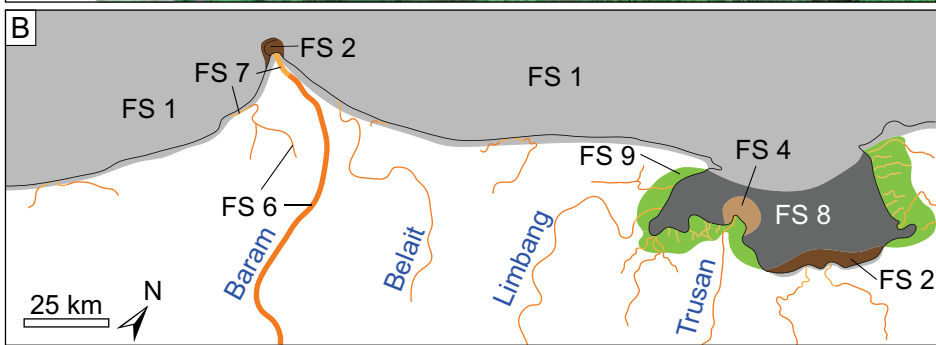
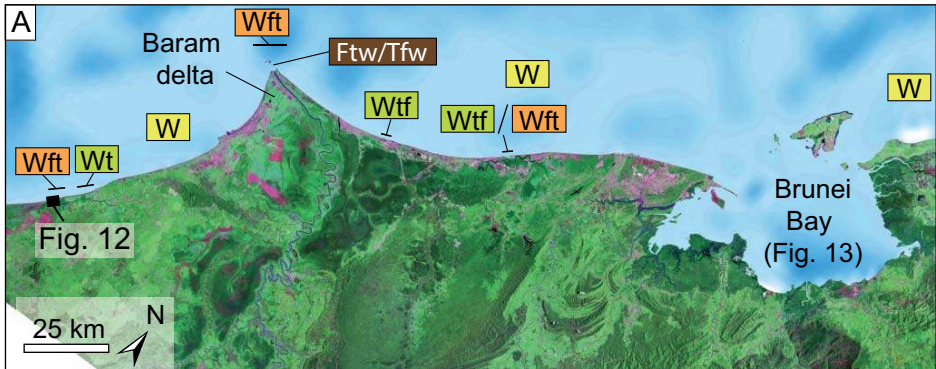
C **FSS 3** Tide-dominated, wave- and river-influenced embayment

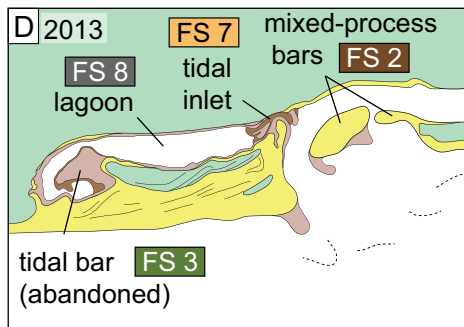
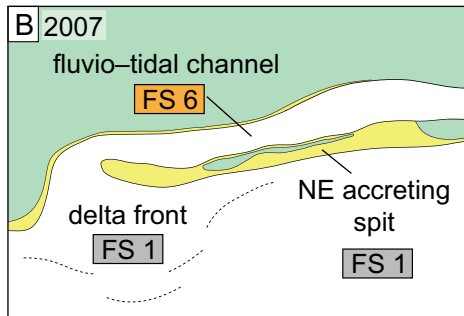




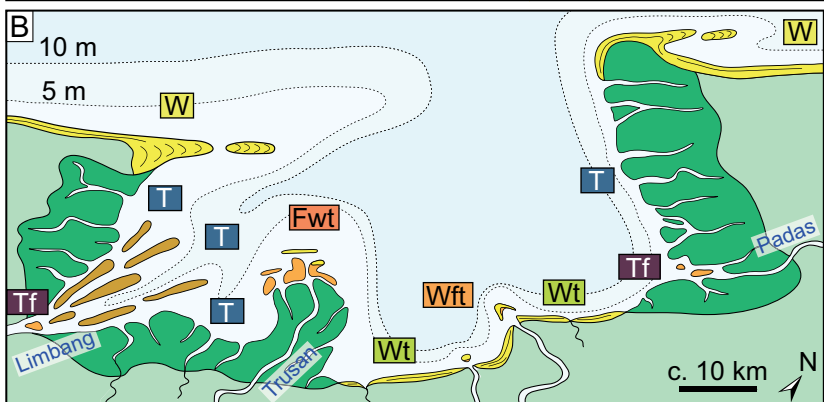
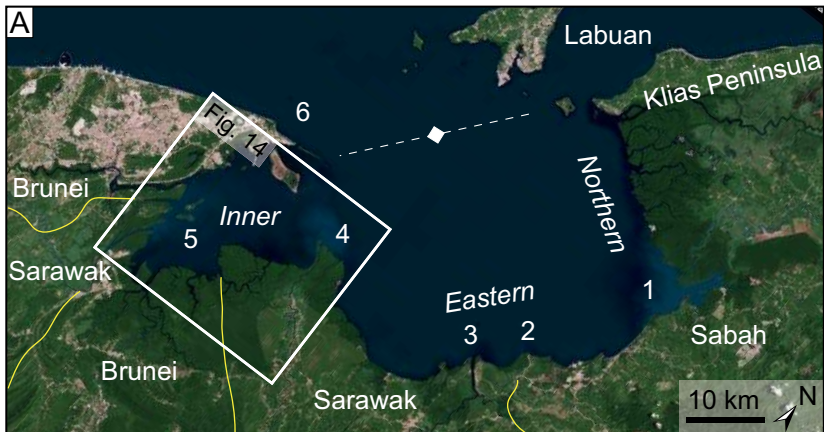




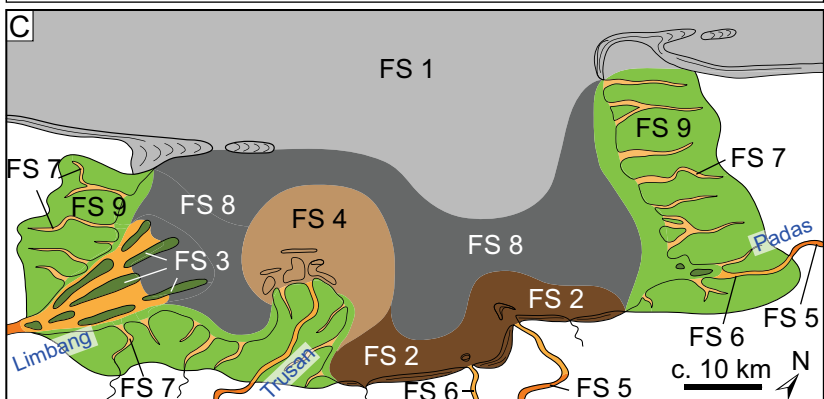


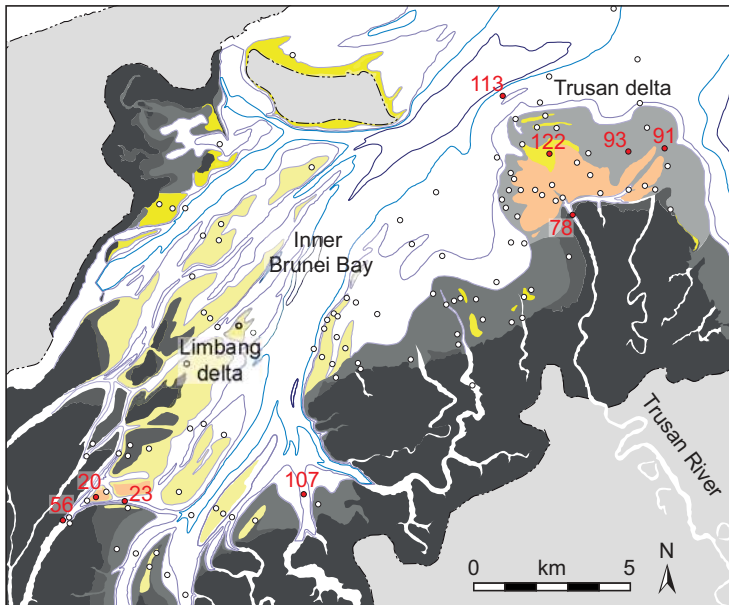


Key	Sandy sediment	Muddy sediment	Vegetation
	above low tide subtidal	subtidal	<i>Casuarina</i> -dominated



- | | |
|---|-----------------------------|
| Wave-generated lobe, spit or strandplain | Subtidal to intertidal bars |
| Mouth bars, levees | Intertidal mangrove swamps |
| <i>Casuarina</i> -dominated coastal plain | |





Key:

Depositional environment

□ SUBTIDAL

■ Wave-generated spits or bars

■ Mouth bars or levees

■ Delta front

■ Intertidal bars

Tidal flat

■ Unvegetated mudflats (above SLW)

■ Unvegetated mudflats (above MLW)

■ Mangrove swamp

□ SUPRATIDAL

Bathymetry contour

⋯ Spring high water (SHW)

— 1 m contour (spring low water, SLW)

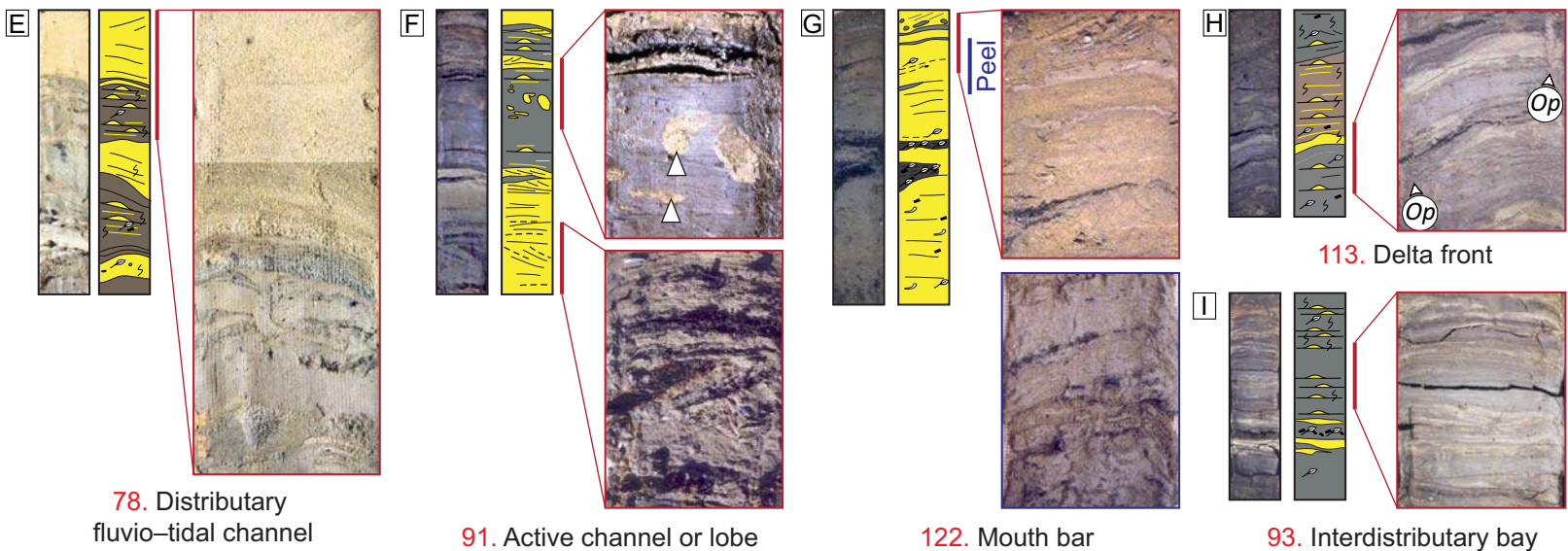
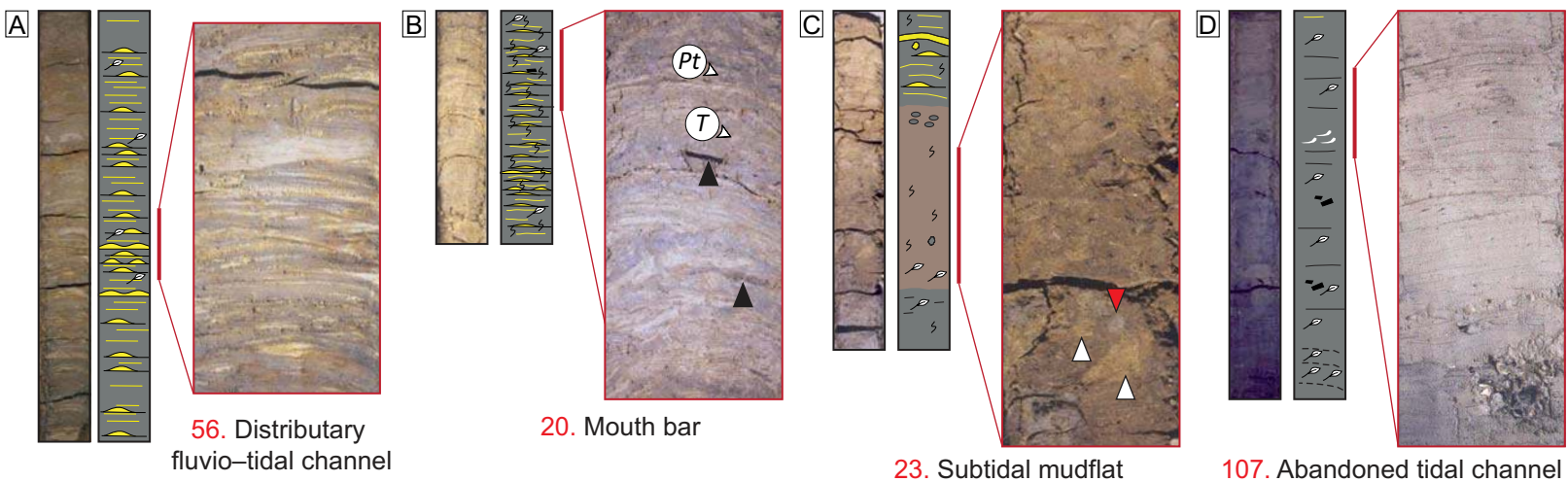
— 2 m contour

— 5 m contour

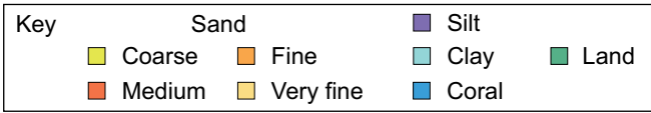
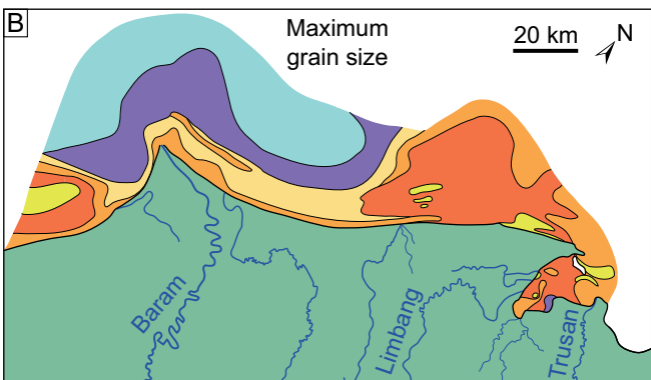
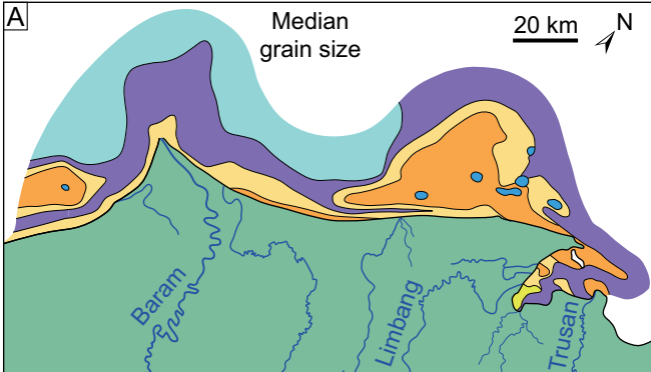
— 10 m contour

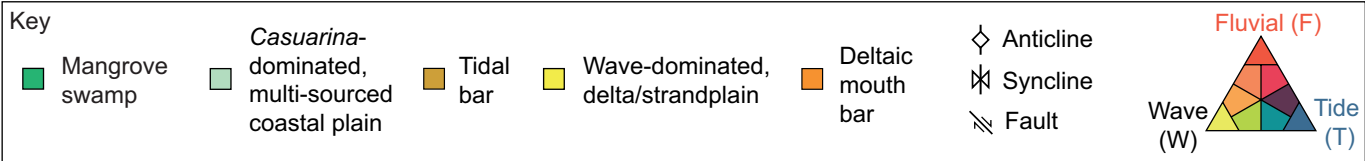
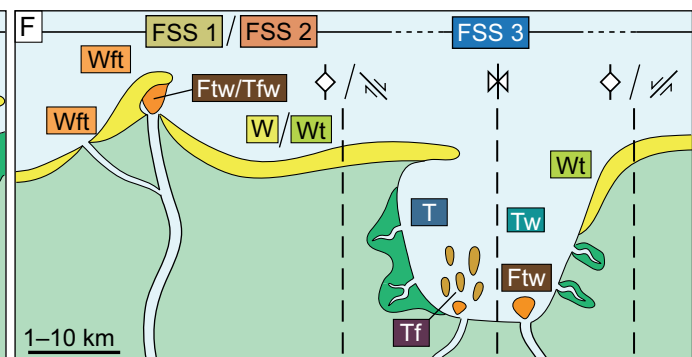
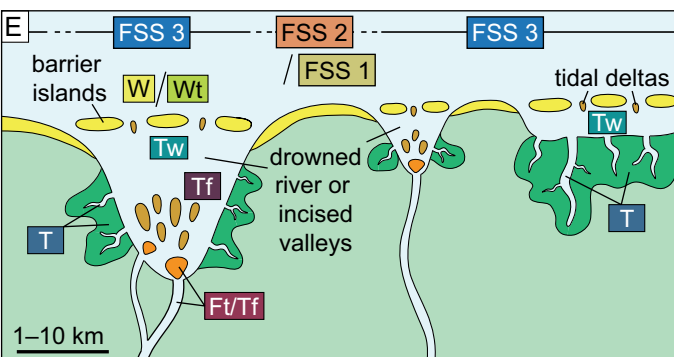
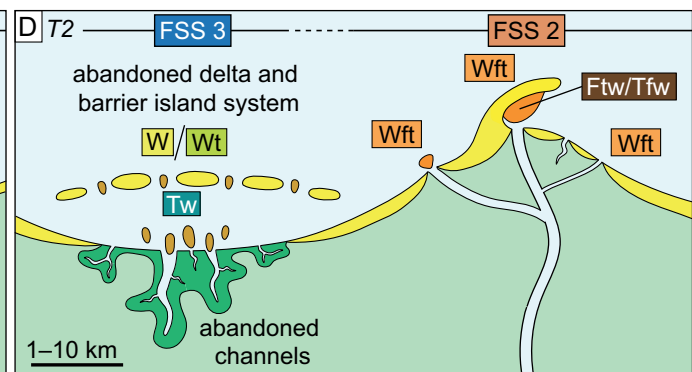
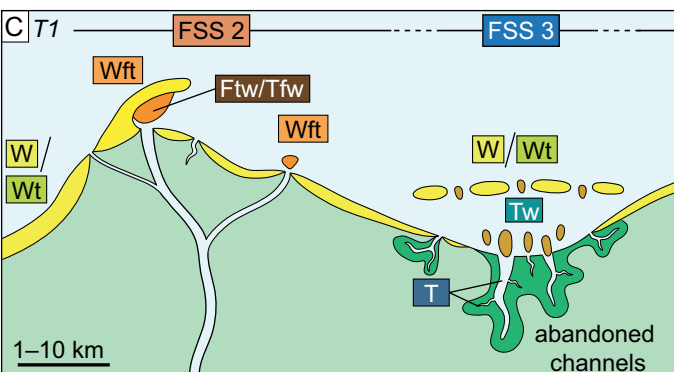
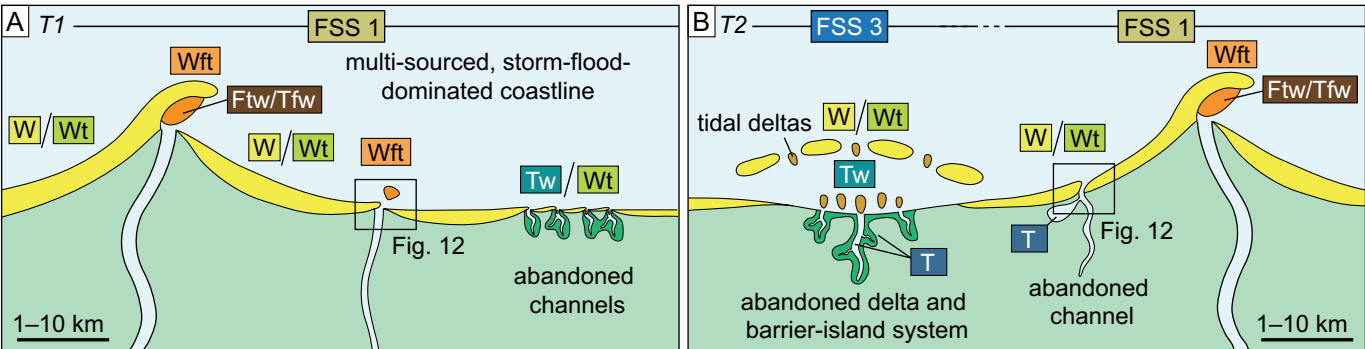
○ Vibracore location

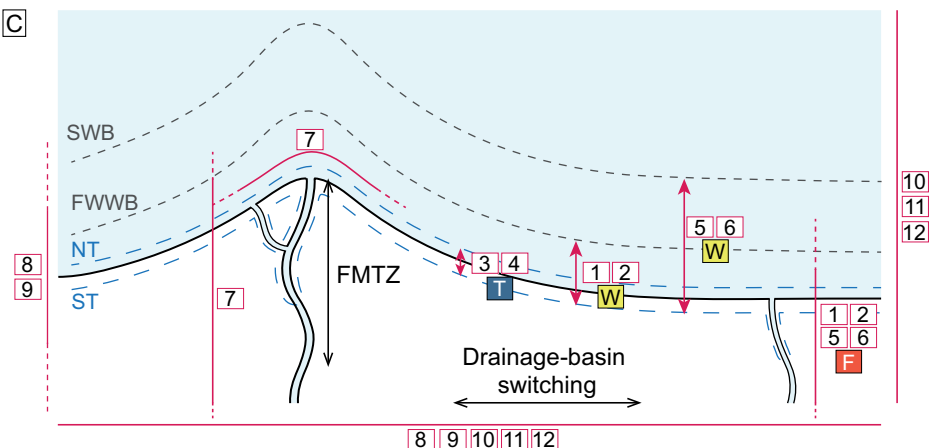
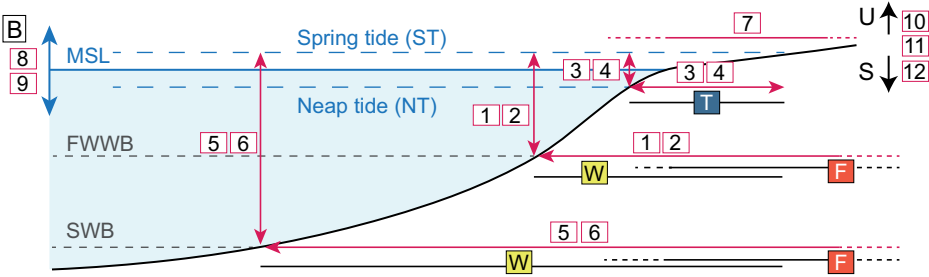
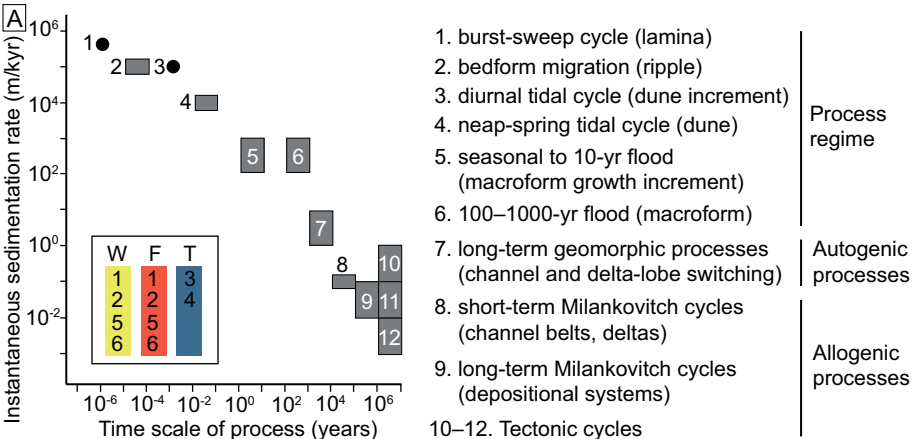
● Vibracores studied








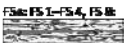



Key					
10 cm	Sandstone	Wavy bedded sandstone	Mudstone intraclasts	Mollusc shells or shell fragments	
	Muddy sandstone	Lenticular sandstone	Coal fragments	Mud-filled <i>Thalassinoides</i>	
56 Core number	Mudstone	Sandstone laminae	Carbonaceous debris	Sand-filled <i>Thalassinoides</i>	
		Lamination	General bioturbation	Organic-carbon debris	







Facies	Grain Size	Sand:Shale Ratio	Sandstone Dimensions	Mudstone Dimensions	Description	Biogenic Structures	Process Interpretation	Environment Interpretation	Facies Sketch
F1 Coal	Coal, minor silt- st- silt	N/A	mm-cm thick, dm wide	N/A	Dark brown to black, moderately dull, minor bright vitreous layers, irregular silt- st patches	N/A	Mangrove-dominated organic-carbon soil/past, low clastic sediment supply	Tropical, intertidal, tide-dominated, mangrove-vegetated, lower coastal plain	F1  10 cm
F2 Structureless mudstone	ms, minor silt- st	F2a-bc <0.2 typically <0.1	F2a-bc c. 5-50 m thick, c. 1-100 m wide	F2a-bc 5-30 m thick >300 m wide	F2a: Massive and variably bioturbated ms, common carbonaceous debris, F6-F7 interbeds F2b: Massive, abundant carbonaceous debris, mangrove roots, intimately bioturbated silt	F2a: BI 0-6, Indistinct and F6, P, T6, C6, As F2b: BI 4-6, Indistinct and dm-scale T6	F2a: Suspension settling and/or high-energy fluid-mud deposition F2b: Suspended-mud deposition	F2a: Storm-dominated prodelta and/or offshore-shelf or embayment F2b: Mangrove-vegetated intertidal region, tide-dominated, wave-protected embayment	F2a  10 cm F2b  10 cm
F3 Laminated mudstone	ms, minor silt- st	<0.2 typically <0.1	sub-mm-mm thick, cm-dm wide	0.1-3 m thick, m-scale wide	Laminated ms with wavy parallel streaks and stacked ripple-cross-lamination of silt- st, carbonaceous debris	BI 0-2, low diversity Khalafoua F6, P, T6, C6	Variable-energy storm-flow—low-energy-suspension settling, high-energy wave-enhanced, sediment-gravity flow and/or fluid mud	Storm-dominated prodelta and/or offshore-shelf to distal (or near-rich) delta front and/or flanking strandplain	F3  1 cm
F4 Muddy heterolithic	F4a-bc Silty ms and silt- st	F4a-bc 0.3-0.5	F4a-bc 0.1-5 cm thick, c. 10-100 m wide	F4a-bc 0.1-5 cm thick and c. 1-100 m wide packages	F4a: Wavy lenticular bedded, oscillation and combined-flow ripples, wavy to parallel lamination, cm-dm scale scours, minor ms drapes F4b: Current ripples (bidirectional) clastic, common ms and carbonaceous drapes and clasts	F4a: BI 1-2, BI 4-5 locally silt—R, C6, P, R ms—P6, T6, P F4b: BI 1-2 BI 4-5 locally silt—P6, R, C6, C6, J ms—P, T6, G6	F4a: Fluctuating energy and/or sediment supply; erosional, oscillation-dominated combined flow, possible fluid-mud drapes F4b: As F4a but current-dominated flow	F4a: Storm-dominated prodelta and/or offshore-shelf to distal delta front and/or flanking strandplain F4b: Tide- and river-influenced channel and/or bar and/or delta, low wave energy	F4a  10 cm F4b  10 cm
F5 Sandy heterolithic	F5a-bc silt- st and silty ms	F5a-bc 0.5-0.8	F5a-bc 0.1-10 cm (beds), 2-5 m thick (units)	F5a-bc 0.1-3 cm, <1 m wide drapes, 1-30 cm thick and 1-100 m wide beds	F5a: Wavy and flexer bedding, combined-flow ripples and wavy planar lamination, occasional oscillation ripples, minor ms and carbonaceous drapes and clasts F5b: As F5a but current ripples (bidirectional) clastic and common ms and carbonaceous drapes and clasts	F5a: BI 1-3, BI 3-5 locally, T6, C6, C6, T, F, R, L6, As F5b: BI 1-3, BI 3-5 locally, small-scale P, P, C6, R, T, T6, C6, C6, J6	F5a: Oscillation-dominated, muddy, turbulent-laminar combined flow, variable sediment supply (storm-flood related) F5b: Current-dominated, minor flow reversal (tides), variable energy and/or sediment supply, physicochemical stress	F5a: Storm-dominated delta front and/or flanking strandplain F5b: Tide- and river-influenced channel and/or bar and/or delta, low wave energy	F5a  10 cm F5b  10 cm
F6 Sandy cross-stratified sandstone	silt- st	>0.8 typically >0.9	0.1-3 m thick beds and 1.6-3.6 m thick bedsets, >300 m wide (c. km-scale)	<0.3-2.8 m thick and >300 m wide F2-F4a interbeds	Low-angle (< 20°), large-wavelength (> 10 m) SCS, sandy discontinuities, common SCS downlap and asymmetry, sharp erosional base, cm-m-scale gutter casts, sharp tops	BI 0-1, BI 1-2 near bed tops, C6, P, P, R, L6	Oscillation-dominated combined flow, high sedimentation rates, frequent erosion	Storm-dominated (nearshore) distal to proximal delta front and/or flanking strandplain	F6  10 cm

Facies	Grain size	Sand-Shale Ratio	Sandstone Dimensions	Mudstone Dimensions	Description	Stratigraphic Structures	Process Interpretation	Environment Interpretation	Facies Sketch
F7 Hummocky cross-stratified sandstone	silt- of silt	>0.8 typically >0.9	0.1-1 m thick beds, 1-3.6 m thick and >300 m wide bedsets	<0.3-2.8 m thick and >300 m wide F2-F4a interbeds	As F6 but includes dm-scale convex-up lamination (hummocks)	B1 B-1, B11-1-2 near bed tops, Op, P, Pt, Pc, fu	Oscillation-dominated combined flow, increased aggradation vs. erosion (cf. F6)	Storm-dominated (freshwater) distal to proximal delta front and/or flanking strandplain	F7a: FS 1-FS2, FS 8: 1m
F8 Laminated sandstone	F8a- silt- of silt	F8a- >0.9	F8a- 0.1-0.75 m thick beds, 1-2.5 m thick and >300 m wide bedsets	F8a- dm- m thick laminae F8b: N/A	F8a- Low angle (< 3°) lamination, subtle internal discontinuity surfaces, minor rust and carbonaceous drapes and clasts (FS 1-FS 4, FS 6)	F8a: B1 B-1-3 Op, P, Pt F8b: B1 1-5 Op, P, Pt F8c: B1 D	F8a: High energy, oscillation- dominated combined flow F8b: As F8a but increased physicochemical stress F8c: Upper flow regime, current dominated	F8a: Storm-dominated, delta and/or flanking strandplain F8b: As F8a but increased physico- chemical stress F8c: Low flow regime, current dominated	F8a: e.g. FS 1 F7-F8 F2-F4a F8a: FS 2-FS 3 30 cm F8-F7c F8a: 30 cm FS 3, 6-7 FS 4-7 FS 4-6 F8a: FS 1-FS 2 30 cm
F9 Trough cross-stratified sandstone	F9a- silt- of silt	F9a: >0.9	F9a: 10-50 cm thick, <15 m wide lenses (within F8a- bedsets)	F9a- cm- m thick and cm-dm wide	F9a: 5-80 cm cross-sets, 20-25° scoop-shaped foresets, occasional bidirectionality, rust and carbonaceous drapes and clasts F9b: As F9a with F10a tocsets F9c: As F9a but predominantly sub-parallel and unidirectional foresets	F9a: B1 B-1-3 Op, P, Pt F9b: B1 B-1, sporadic B1 3-3, P, Pt, P, S, Op F9c: N/A	F9a: Current-dominated, tidal, fairweather wave and/ or storm flow, minor flutic or suspended mud deposition F9b: As F9a but common mud deposition (fluvial and/ or tide-energy variability) F9c: Current- and freshwater-dominated	F9a: Shallow marine, tidal, fairweather wave and/or storm reworking F9b: Fluvial-tidal channel and/or delta and/or bar F9c: As F9b but river-dominated	F9a: FS 1-FS 2 30 cm F9a: FS 3, FS 6-FS 7 30 cm F9c: FS 4-FS 5 30 cm
F10 Rippled sandstone	F10a- silt- of silt	F10a- >0.8	F10a- 0.1-0.3 m thick, c. 1-300 m wide	F10a- cm- dm thick, cm-dm wide drapes F10b: N/A	F10a: Wave and combined-flow ripples, minor current ripples and mud drapes F10b: Current ripples, common bidirectional, minor combined-flow and climbing- current ripples, rust and carbonaceous drapes and clasts F10c: Climbing current ripples, minor carbonaceous drapes	F10a: N/A F10b: B1 B-3, sporadic, P, Pt, P, S, As, B F10c: N/A	F10a: Oscillation- to combined-flow-dominated, possible fluid-mud deposition F10b: Current-dominated, tides (bidirectional and stack-water mud) and river flooding cyclicity F10c: Current-dominated, high sediment supply	F10a: Proximal delta front and/or flanking strandplain F10b: Fluvial-tidal bar within channel or shallow-marine tidal reworking F10c: River-dominated bar within channel	F2- F10a F10a: FS 1-FS 2 30 cm F10b: FS 3, 6-8 20 cm F10c: FS 4-FS 5 20 cm
F11 Conglomerate	F11a- granule, pebbles and rare cobbles, of silt matrix	F11a: 0.4-0.8	F11a- 5-30 cm thick, dm-m wide	F11a- N/A	F11a: Mudstone intraclasts (granules to pebbles), rare sandstone extraclasts (granules to cobbles), typically matrix supported, associated erosional base F11b: As F11a but sandstone-dominated clasts	F11a: B1 B-1-3 P, Pt F11b: N/A	F11a: High-energy erosion and deposition, mudstone- dominated source F11b: As F11a but sandstone-dominated source	F11a: Tide-dominated and fluvial-tidal channel lags (FS 6-FS 7) and high energy erosive storm flows (FS 1-FS 3) F11b: River-dominated fluvial-tidal channel lag and high-energy flows	F11a: FS 1-3, 6-7 5 cm F11b: FS 5-FS 6 cm

Facies Succession	Diversions and Log	Facies and ichnofauna	Associations and Figures	Environment and Process Interpretation	
FS 1 Sander-upwards, mudstone-dominated and sharp-based, swaley cross-stratified, sandstone-dominated units		F6 F8a F4a F3 F2a F7 F9a F10a F11a	FW: BI 0-5 <i>P, T, Th, Ch, R, Pa</i> S: BI 0-2 <i>Op, Pt, Po</i>	Gradually or abruptly overlies FS 1-3, 5-8 Overlain by FS 1, 5-7 abruptly or FS 1, 8 gradually Figures 2, 9	Fully marine, storm-dominated, open coastline delta front and flanking shoreface
FS 2 Sander-upwards, variably bioturbated heterolithic to swaley cross-stratified, sandstone-dominated units		F6 F8b F8a F5a F4a F3 F2a F10a F9a F11a	BI 1-5, highly variable abundance and diversity <i>Op, Th, P, Pa, As, Ph, Cb, No, Sk</i>	Overlies FS 2-3, 6-9 gradually or FS 1-2 abruptly Abruptly overlain by FS 2, 6-9 or gradually by FS 1-2 Figures 2, 3, 9, 10	Mixed-energy, storm- to river-dominated, tide-affected (?) delta and flanking shoreface, open or embayed coastline
FS 3 Upward-coarsening, muddy to sandy heterolithic units		F5b F4b F9b F10b F3 F4a F8c F8a F10a F11a	BI 1-2, locally BI 3-4, moderate diversity <i>P, T, Th, Cq, R, Pt, Sk</i>	Gradually or abruptly overlies and overlain by FS 1-2, 6-9 Figures 4, 1B	Prograding tide-influenced/-dominated bars and/or deltas within a relatively low-wave-energy embayment or tide-dominated, fluvial-tidal channel
FS 4 Upward-coarsening, sparsely bioturbated, heterolithic to sandstone-dominated units		F9c F8c F8d F10c F3 F6 F8a F2a	BI 0-1 Absent to minor, mm-scale simple, low diversity (e.g. P)	Gradually overlies FS 8 Abruptly overlain by FS 4, 6-8	River-dominated, wave- and tide-affected mouth bar and/or delta
FS 5 Erosionally based, fining-upwards sandstone-dominated to muddy heterolithic units		F9c F8c F8d F10c F4b F11b	sst: absent mst: BI 0-1 <i>P, Pa, Pt, micro-Op, fu</i>	Abruptly overlies FS 4-8 Overlain gradually by FS 8 and abruptly by FS 1-2, 8	River-dominated channel (and abandonment), single-story (3-5 m thick) and multi-story (10-70 m thick)
FS 6 Erosionally based, fining-upwards sandstone-dominated to sandy and muddy heterolithic units		F5b F9c F9b F4b F10b F11a F8d F8c F10a	BI 0-2 <i>P, Pa, Pt, Sk, Op, cb</i>	Abruptly overlies FS 6-8, 1-2 Overlain gradually by FS 1-3, 8 and abruptly by FS 1-2 Figures 5, 9, 10	Tide-influenced fluvial channel (and abandonment), single-story (3-5 m thick) and multi-story (10-70 m thick)
FS 7 Erosionally based, fining-upwards, heterolithic-dominated units		F5b F9b F4b F10b F11a F9d F9c F4a	BI 0-3, locally BI 4 <i>P, Pa, Pt, Sk, Op, cb</i>	Abruptly overlies FS 8-9, 2 Overlain gradually by FS 8-9 or abruptly by FS 1-2, 8-9 Figures 5, 10	Tide-dominated subtidal channel (sand- and mud-dominated)
FS 8 Laminated to massive mudstone units with sandy interbeds		F3 F2a F4b F7b F5b F4a F2b F5a I /	BI 0-2, locally BI 3-5 <i>P, T, Th, Pa</i>	Gradually or abruptly overlies FS 2-7, 9 Overlain abruptly by FS 5-7 and gradually by FS 1-4, 9 Figures 5, 10	Variably tide- and storm-dominated, river-influenced, marginal-marine and brackish embayment or abandoned fluvial-tidal channel
FS 9 Massive, carbonaceous mudstones units with minor sandy laminae and interbeds		F2b F4b F5b F1	Th, P Indistinct & rooting BI 4-5	Gradually or abruptly overlies FS 6-8 Overlain gradually by FS 8 and abruptly by FS 1-3, 6-8 Figures 5, 10	Tide-dominated, mangrove-vegetated, intertidal to subtidal flat in a relatively low-wave-energy, marginal marine embayment